CONTRACT SERIAL NO. 79213-01-SQ
CONTRACTOR: ORTECH INTERNATIONAL
CONTRACT DSS REQ'N NO. 23440-7-9213

Investigation of the Mechanism of Hydration in High Volume Fly Ash–Portland Cement Binders

DSS Contract Serial No. 23440-7-9213/01SQ
Report No. 64-10919

FINAL REPORT

for

CANMET – MSL Division
Energy Mines & Resources Canada
555 Booth Street
Ottawa, Ontario
K1A 0G1

Attention: Dr. V.M. Malhotra

Prepared by:

E.E. Berry, Ph.D.
R.T. Hemmings, Ph.D.
B.J. Cornelius

June, 1989

81 pp

MICROMEDIA

ORTECH
INTERNATIONAL
2395 Speakman Drive
Mississauga, Ontario L5K 1B3
(416) 822-4111
Telefax (416) 823-1446

60 Years of Service to Industry

ORTECH Corporation

Terms and conditions on reverse.

We, ORTECH Corporation, conducting business as "ORTECH International", stipulate that this document is subject to the following terms and conditions:

1. Any proposal contained herein was prepared for the consideration of the addressee only. Its contents may not be used by nor disclosed to any other party without our prior written consent.

2. Any testing, inspection or investigation performed by us will be conducted in accordance with normal professional standards. Neither we nor our employees shall be responsible for any loss or damage resulting directly or indirectly from any default, error or omission.

3. Any report, proposal or quotation prepared by us refers only to the particular material, instrument or other subject referred to in it. No representation is made that similar articles will be of like quality.

4. No report issued by us shall be published in whole or in part without our prior written consent.

5. Our name shall not be used in any way in connection with the sale, offer or advertisement of any article, process or service.

6. We reserve the right not to commence and/or continue any work until payment arrangements satisfactory to us are established.

SUMMARY

This report describes work on an investigation of high-volume fly ash (HVFA)-Portland cement (PC) binders, the physical and chemical properties of which have been characterized up to 365 days of curing. At appropriate ages, specimens were examined from two series of superplasticized mortars or pastes (one series made with Portland cement only, the other containing high-volumes of fly ash substituted for cement). Physical investigations were made of compressive strength development, pore structure by porosimetry, and morphology by scanning electron microscopy. Chemical examination was conducted for solid phase composition and degree of hydration by X-ray diffraction and thermal analysis, and for pore-fluid composition by high pressure extraction and analysis.

Conclusions as to the mechanism of hydration and strength development in the HVFA materials, based on their observed physical and chemical characteristics, are as follows.

Physically, the HVFA mortars have excellent long-term strength development, which strongly indicates that the fly ash is undergoing pozzolanic reaction. In addition, the fly ash particles in the HVFA materials promote good densification of the matrix through space-filling and by acting as centres for the growth of cementitious hydrates. Densification is also assisted by the use of superplasticizer to achieve a low water content in the mixes. This results in very low porosity and a micropore structure extending to below 0.02 μm. A unique characteristic of the HVFA pastes, which must be related to the pore structure, is that pore fluids can be extracted up to 365d, whereas this was only possible up to 7d for the reference PC pastes.

There is significant evidence that up to 365d the cement in the HVFA pastes is not fully hydrated and that the ash is participating chemically in both early (sulphoaluminate) and late (aluminosilicate) hydration reactions. This is shown by acceleration of cement hydration, progressive calcium hydroxide consumption, and high levels of bound water. Ettringite (AF_t) has been identified as a product of the early hydration of the fly ash. It has not been possible to identify long term hydration products which appear to be non-crystalline.

On the basis of thermodynamic considerations, the pore fluid chemistry in the HVFA system has been found to be substantially different from the reference PC system. The main difference appears to lie in control of calcium solubility. There also appears to be a mechanism for long term binding of OH, Na and K in the HVFA pastes. The pore fluids in both the HVFA and PC pastes are extremely concentrated, being best considered as ~1M solutions of sodium and potassium hydroxides. This is considered to be a significant factor in promoting attack on the fly ash glass. There are also indications of chemical involvement (complexation) of the superplasticizer in the pore fluid system.

Although the fly ash spheres appear in the SEM to be relatively unetched up to 365d, there is good evidence that they are, in fact, still undergoing chemical reactions. Drawing on

similarities with acid-leached fly ash residues, the term "pseudomorphic" has been introduced to describe the fly ash spheres in this condition, in recognition of this retention of their basic spherical particle morphology after having been chemically changed.

A mechanism for the pozzolanic reaction between fly ash and Portland cement has been proposed in terms of a two-step process involving (a) depolymerization/silanolation of the glassy constituents of the ash by the highly alkaline pore fluids, by analogy with the same process well-established by glass science in conventional glasses, followed by (b) reaction between solubilized silicate and calcium ions in solution to form C–S–H.

A number of characteristics of the fly ash pastes undergo discontinuous changes during the period 28 to 90d, manifested by the appearance of maxima or minima in time-dependent parameters observed during this period. Notable in this respect are:

- total pore volume
- the quantity of bound water relative to cement content
- the quantity of $Ca(OH)_2$ in the paste
- pore water saturation to $Ca(OH)_2$
- Na, K, SO_4 and OH concentrations in pore water

It is clear that major changes in chemical and physical properties occur in the pastes during this time period. These may or may not be inter-related; present data do not permit further conclusions on this issue, although further investigation is clearly required.

The overall conclusion is that in the HVFA system, physical and chemical factors combine at all ages to densify and bind the paste. In the early stages, the physical effect of space filling and the chemical contribution to sulphoaluminate production are important; whereas, in the longer term, the pozzolanic hydration reactions dominate as binder is generated by reaction of fly ash particles to replace the cement deficiency.

E.E. Berry, Ph.D.
Consultant

C.S. Gibbons, Ph.D.
Manager
Inorganic Materials Centre

R.T. Hemmings, Ph.D.
Consultant

CONTENTS

Section **Page**

1. INTRODUCTION 1

2. EXPERIMENTAL METHODS AND RESULTS 2
2.1 Materials 2
2.2 Mix Proportioning 2
2.3 Characterization of Pastes and Mortars 4
Strength Development of Mortars 4
Scanning Electron Microscopy 4
Porosimetry 4
X-ray Diffraction Analysis 5
Thermal Analysis 5
Pore Fluid Extraction and Analysis 6

3. DISCUSSION 7
3.1 Possible Roles for Fly Ash in HVFA Materials 7
3.2 Strength Development of Mortars 8
3.3 Physical Microstructure of Pastes and Mortars 9
Morphology and Microchemical Features 9
Pore Structure 10
3.4 Solid Phase Identification in Hydrated Pastes 11
3.5 Extent of Hydration: Calcium Hydroxide and Bound Water 13
3.6 Pore Fluid Chemistry and Paste Hydration: Theory 15
The Origin of Ionic Species in Pore Fluids 15
Changes in Solution Composition During Hydration 16
Thermodynamic Relationships in Pore Fluids 17
3.7 Pore Fluid Chemistry and Paste Hydration: Mechanistic Implications 18
Pore Fluid Composition 18
Calculation of Aqueous Phase Compositions 19
Early Age Supersaturation 20
Formation of Ettringite and Gypsum 21
Late Age Supersaturation 23
3.8 Fly Ash Hydration 24
Short Term (Sulphoaluminate) Reactions 24
Long Term (Pozzolanic) Reactions 25

4. CONCLUSIONS 28

References 30
Tables 34
Figures 47

1. INTRODUCTION

In a recently published paper, Malhotra [1] described the development of high-strength concretes incorporating large volumes of fly ash. Further data on these materials — which are termed high-volume fly ash (HVFA) concretes — were presented at a recent CANMET seminar [2].

The basic concept of the HVFA materials is to produce structural concretes in which fly ash comprises more than 50% of the total cementing material (i.e. Portland cement and fly ash). By careful selection of mix proportions and the use of chemical superplasticizers, HVFA concretes produced at CANMET have been shown to develop compressive strengths of the order of 30–40 MPa by 28 days with relatively high early-age strength (10–15 MPa at 3 days). The significant feature of these concretes is their low Portland cement content (~150 kg/m^3), thus permitting them to be produced at less cost and less energy demand than conventional Portland cement concretes. Overall, these materials present a considerable advance in the use of fly ash in concrete.

In addition to their composition, HVFA concretes are unusual in respect of two properties:

- They attain high-strength at exceptionally reduced Portland cement content.
- The elastic modulus of HVFA concretes is some 10–20% greater than for concretes of comparable strength made using Portland cement alone.

These properties indicate that HVFA concretes probably differ in microstructure from conventional concretes.

The objective of the present investigation has been to develop an understanding of the mechanisms responsible for bonding in HVFA materials. The study has been directed to an examination of the microstructure and hydration chemistry of some high-volume fly ash pastes and mortars prepared with Portland cement and Lingan fly ash at various ages of curing ranging from 2 hours to 365 days. This Lingan fly ash was selected since it has been extensively characterized in recent work by the present authors [3–5], and is the same source used in the CANMET work [1,2].

At appropriate ages, specimens of mortars or pastes have been examined physically for compressive strength, pore structure by porosimetry, and morphology by scanning electron microscopy; and chemically for solid phase composition and degree of hydration by X-ray diffraction and thermal analysis, and for pore fluid composition by high pressure extraction and analysis.

2. EXPERIMENTAL METHODS AND RESULTS

2.1 Materials

The cement used in this study was a fresh, CSA Type 10 Portland cement (PC) supplied by CANMET that originated from Canada Cement Lafarge (Woodstock Plant), The chemical and physical characteristics of the cement are summarized in Table 1. The cement can be considered to be typical of its class with 3.0% SO_3, moderately high alkali content (total ~1.1% as Na_2O), and the following calculated (Bogue) clinker components: C_3S, 51.6; C_2S, 22.0, C_3A, 6.1; and C_4AF, 8.5%. X-ray diffraction analysis of the cement indicated that the SO_3 was present largely in the form of anhydrite ($CaSO_4$) with some gypsum ($CaSO_4 \cdot 2H_2O$) and possible hemihydrate ($CaSO_4 \cdot 0.5H_2O$). The cement also contained a small quantity of calcium carbonate (~2.3% by thermogravimetric analysis) permitted under CSA Standard CAN3-A5-M77.

The fly ash originated from the Lingan Generating Station, Nova Scotia, and was the same as used in previous studies by the authors [3-5]. Chemically (Table 1), it can be classified as a bituminous fly ash with a high iron content (24% Fe_2O_3), and with low levels of carbon (1.9% C) and sulphur (1.3% SO_3). Mineralogically, the ash has a moderately low glass content of ~58%, the balance being comprised of quartz (~9.6%), mullite (~20%), spinel, (~4.5%), and hematite (~5.4%). As received from the power plant, the ash has good fineness (86.4%, -45 μm; mean size, 10.1 μm) and is a good pozzolan (ASTM C311 28d activity index with Portland cement, 83.8%).

The superplasticizer selected for the study was DISAL FSP™ and was used as supplied by Handy Chemicals, Montreal, in the form of a premixed aqueous solution containing 41.2% by mass total solids. Chemically, it is a sodium salt of a sulphonated naphthalene-formaldehyde condensate (Table 2) with significant levels of sodium (13.8% Na_2O) and sulphur, mostly as sulphonate (27.8%) but with some free sulphate (15,500 mg/L SO_4^{2-}).

The sand used for the preparation of the mortars was a standard Ottawa high quartz silica grade conforming to the requirements of ASTM C109. The water used for the hydration of the pastes and mortars was of deionized laboratory grade which had been boiled to remove carbon dioxide. The pH of the water was typically 6.9–7.1 with the following trace element content: Si, 0.05; Al, <0.02; Fe, <0.02; Ca, <0.02; Mg, <0.02; Na, <0.5; K, <0.1 μg/mL.

2.2 Mix Proportioning

The objective in selecting mix proportions for the mortars and pastes for this study was to produce materials of similar composition to the cementing constituents in the superplasticized fly ash concretes studied by CANMET [1,2]. The use of more than 50% of fly ash as a cementing material in conjunction with Portland cement represents such a significant departure from 'normal' concrete proportioning practice that it presents a problem in discussing the influence of composition on concrete performance.

It is common practice in considering fly ash concrete mixtures to discuss their properties in comparison with a 'control' concrete of conventional composition and similar properties. The problem with the HVFA materials is that there is no 'control' concrete with which comparisons can be made. It has long been advocated by some researchers that fly ash concretes should be considered as 'new materials' rather than as derivatives of some hypothetical 'normal' concrete. In cases where fly ash has been substituted for 10-20% of Portland cement in an otherwise typical concrete mix, the need for this approach has not been strongly felt, nor has it been commonly followed. When, as is the present case, some 58% of the 'cementing material' is fly ash, clearly the concept of substitution is no longer valid.

In published work on HVFA concretes, Malhotra [1,2] has presented performance data from studies in which no 'control' concrete was included in the experimental design, the strength data of HVFA concretes being presented to stand alone. In the present study, and to provide some basis for comparison, some pastes and mortars were prepared using Portland cement alone. These should not be regarded as 'control' specimens in the familiar sense; but, rather, they are included as points of reference from which significant aspects of the properties of the high-volume fly ash mixes can be recognized.

Mortars: The proportions used in preparing the mortars and pastes are shown in Table 3. To establish the baseline performance of the Portland cement with that considered normal for a commercial cement, a series of reference mortar samples was prepared according to the requirements of ASTM C109, using Portland cement as the sole binder, without incorporation of superplasticizer. Superplasticized mortars were prepared containing either Portland cement as the sole binder, or a mixture of Portland cement and fly ash. These were used to compare the strength development of Portland cement (PC) systems with Portland cement–fly ash (PC–FA) systems at high fly ash loadings. Standard 2-inch mortar cubes were prepared according to the mix proportions given in Table 3. The specimens were cured at 21°C (± 1°C) and 100% humidity until the time of testing. A constant value of w/(c+f) = 0.30 was maintained for the superplasticized mortars. This resulted in a mixture with zero flow for the PC_{sp} mortar and a flow of 37 for the $PC–FA_{sp}$ mortar.

Pastes: A reference paste with w/c = 0.30 was prepared to simulate the paste in a superplasticized PC concrete without fly ash. To simulate conditions in a superplasticized concrete incorporating both Portland cement and fly ash, a paste with w/(c+f) = 0.30 and a 58% mass replacement of Portland cement by fly ash was selected. The quantity of added superplasticizer was based upon the quantity of Portland cement used in each mixture. It was maintained at a level of 1.05 g of superplasticizer per 100 g Portland cement. This approach is somewhat arbitrary in that it implies that the superplasticizer acts only on the Portland cement, even in the presence of fly ash. The approach was selected to maintain similar mixture proportions to those used in the CANMET work [1,2].

The water introduced with the superplasticizer (41.2% solids) was included in the calculation of the w/c ratio for the pastes. A series of pastes of each type was prepared. Exposure to air was controlled during preparation and handling to minimize the effects of carbonation. All paste samples were sealed in plastic molds (~2.5 cm diameter by 5 cm length) and stored at 21°C (±1°C) until the time of testing.

2.3 Characterization of Pastes and Mortars

A range of physical and chemical techniques was used to examine the development of microstructure in the reference and HVFA systems over a 1 year period. In view of their greater simplicity and ease of handling, the emphasis in this work has necessarily been on the paste systems. The experimental methods and conditions used are summarized as follows.

Strength Development of Mortars

Strength development data for the mortar specimens defined in the previous section and Table 3 were obtained at curing ages of 1d, 3d, 7d, 28d, 56d, 90d and 365d and are given in numerical form in Table 4. The rates of strength gain of the three mortars are compared graphically in Figure 1.

Scanning Electron Microscopy

The development of morphology and microchemical features in the PC and PC-FA pastes was monitored at five curing ages (10h, 3d, 28d, 90d and 365d) using scanning electron microscopy and energy dispersive X-ray analysis (SEM-EDXA). Instruments used included a SEMCO Nanolab 7 equipped with a Kevex 7000 EDXA, a Hitachi S520, and a Hitachi S2500.

Samples from each curing age were prepared in the same manner as was employed for the porosimetry samples (see below) and stored in a nitrogen atmosphere prior to examination. The samples were then carbon coated and examined by SEM-EDXA. Representative scanning elecron micrographs of the hydrating pastes are shown in Figure 2. For comparison with the paste systems, micrographs of fracture surfaces from selected PC–FA mortar specimens were obtained and are given in Figure 3.

Porosimetry

Duplicate samples of the PC and PC-FA pastes were analysed by mercury intrusion porosimetry using a Micromeritics Autopore 9200 instrument. A small portion of each sample (~0.5-1.0 g) was selected such that all surfaces were free of the mold-wall impression. Sample preparation to arrest hydration was carried out by a technique developed at ORF [6,7] which is a modification of the freeze-drying technique described by Orr [8]. A small fragment (~0.5 cm^3) fractured from the paste was carefully placed in a bath of dry pentane, cooled to approximately -125°C. After 2-3 minutes in the bath, the specimen was carefully removed with tweezers and placed in a vacuum freeze-drying

apparatus to remove all free water. After ~18 hours the specimens were removed and fractured to expose a fresh surface, outgassed under high vacuum and then subjected to mercury intrusion from 1.0 psia to 60,000 psia (corresponding to a pore diameter range of 190 μm to 0.003 μm).

The porosimetry-derived output data for pore area, pore diameter, bulk density, skeletal density and porosity for the pastes are summarized in Table 5 and are based on an assumed contact angle (θ) of 130°. Differential pore-size distribution plots (i.e. dv/dp vs. size) for the pastes are given in Figure 4. Corresponding cumulative pore-size distribution curves are compared in Figure 5.

X-ray Diffraction Analysis

Qualitative X-ray diffraction (XRD) analysis was carried out on automated Nicolet I2 and Philips powder diffractometers using monochromatic CuK_α radiation (35kV, 25mA) to assist in identification of the hydration products formed in the PC-FA_{sp} pastes as compared to the reference PC_{sp} pastes. Pastes were prepared and cured in a way identical with those prepared for the pore-fluid extraction and thermal analysis studies. After curing for 2h, 5h, 10h, 1d, 3d, 7d, 14d, 28d, 56d, 90d and 365 days, specimens were dried by the technique described above and subsequently ground for examination by XRD. The resulting XRD patterns (computer enhanced) are shown in Figures 6 and 7 with major phases identified and relative intensity data summarized in Table 6 and Figure 8.

Thermal Analysis

Immediately following the expression of pore fluids (see below), samples for thermal analysis were recovered from the solid paste residues and ground in dry acetone (two cycles) to arrest further hydration. This was followed by drying to a constant weight at 60°C in dry nitrogen, a procedure which has been shown to closely simulate d-drying conditions. After drying, all storage and sample manipulation of samples was carried out in a dry, CO_2-free nitrogen atmosphere.

Thermal analysis (TGA/DTG) of the prepared specimens was conducted on a Dupont 951 thermogravimetric system operating under the following conditions:

Atmosphere:	N_2 gas	Sample weight:	30-55 mg
Flow Rate:	100 cc/min.	Program Rate	10°C/min.
Temp. Range:	21–1000°C		

Examples of the experimental DTG curves obtained for the pastes are given in Figure 9. Following the general data reduction method previously used at ORF [9], a background correction factor was first determined from the thermal curve of unhydrated PC. This factor was then used in a computer program to generate corrected and normalized calcium hydroxide and non-evaporable water contents (Table 7). For comparison purposes, the numerical data are expressed in terms of grams per 100 g PC and grams per 100 g total binder (i.e. PC + FA). These results are summarized graphically in Figures 10 and 11.

Pore Fluid Extraction and Analysis

At curing ages of 2h, 5h, 10h, 1d, 3d, 7d, 14d, 28d, 56d, 90d and 365 days the pore fluid was expressed from the pastes using a high pressure technique based on earlier work by Longuet [10] and Diamond [11]. A nitrogen blanket was maintained in the apparatus during the expression and handling of the fluid in order to prevent carbonation of the highly alkaline liquid. As a further precaution, all manipulations involving the pore fluids were carried out in apparatus constructed of plastic to prevent possible contamination of the solutions by leached SiO_2 from glassware at high pH. The fluids were immediately diluted to standard volume and analysed for Si, Ca, Al, Na, and K by DC plasma spectrophotometry, SO_4^{2-} by ion chromatography, and pH by titration with standard HCl to the methyl red end point.

The results of the pore fluid analyses are given in raw numerical form for the pastes in Table 8 and in graphical form in Figure 12.

3. DISCUSSION

3.1 Possible Roles for Fly Ash in HVFA Materials

Numerous published sources [12-16] have considered the behaviour of fly ash in normal Portland cement concretes and are useful as a point of reference for this study. Generally, the advantages in using fly ash in concrete are considered to arise from physical changes relating to the rheology of the system — such as improved workability and reduction in the w/c ratio and/or cement factor (the plasticising action) — as well as chemical changes such as reduced heat of hydration, improved sulphate resistance and good long-term strength development due to pozzolanic reactions. For the latter, as pointed out recently by Berry and Malhotra [15], it should be noted that while pozzolanic activity is well established as a phenomenon, it is far from being well understood.

Although HVFA concretes contain relatively little Portland cement, more than 50% of the binder being fly ash, they develop greater strength and exhibit a higher elastic modulus than conventional PC–FA concretes. The objective of this study is to identify microstructural mechanisms that may be responsible for the unexpectedly high strength development in HVFA systems. As a framework for discussing the overall problem and the present data, it is useful to consider first the possible effects that the high volumes of fly ash might have in a highly water-reduced cement system and how these might depart from the behaviour of more normal Portland cement–fly ash systems:

- *Space filling:* The fly ash could simply serve to fill space and densify the paste. At the high fly ash loadings used in HVFA materials, the spherical shape of the ash particles could allow them to pack efficiently and effectively fill space between the irregularly-shaped aggregate particles.

- *Floc breaking:* During the early period after gauging with water, while the system is still plastic, the fly ash particles could act to break up the floc structure of the cement, thereby improving dispersion.

- *Nucleating centre:* Ash particles could act as additional nucleating centres for the growth of cementitious hydrates.

- *Supplementary cement:* Fly ash aluminosilicate glass reacts chemically to produce additional cementitious binder. This reaction — commonly referred to as the 'pozzolanic reaction' — is conventionally described as a reaction between calcium hydroxide and reactive siliceous and aluminous materials (which themselves possess no cementitious value). However, as recently summarized by Helmuth [16], the reaction is undoubtedly more complex than this and requires a more complete understanding.

- *Modifier of cement hydration:* Fly ash could provide additional levels of sulphate or otherwise modify the levels of chemical species (e.g. sodium

and potassium) in the system. These species might accelerate or otherwise change the hydration reactions of the cement. At low w/c ratios (as employed in the HVFA materials), large proportions of cement can remain unhydrated even after extended periods of hydration. The fly ash could act to increase the proportion of cement hydrated.

These potential effects could be manifested in a number of ways which could have both physical and chemical consequences in Portland cement–fly ash systems. It is now of interest to examine the present data for indicators that one or more of these mechanisms might be operative in the HVFA materials. The following properties of the HVFA system are the most likely source of these indicators and are discussed first:

- strength development of mortars
- physical microstructure — morphology and pore structure
- solid phase hydration products
- the extent and nature of hydration as a function of curing age
- composition and chemical relationships in the pore fluids

3.2 Strength Development of Mortars

Portland cement mortars made to standard flow (w/c = 0.46) in accordance with ASTM C109 without either fly ash or superplasticizer (Table 4) confirmed that the cement developed strength in a normal manner, reaching 38.2 MPa (5,546 psi) at 28d and 44.1 MPa (6,400 psi) at 365d, with some 35% of the final strength being developed during the first 24h.

Two series of superplasticized mortar mixes were examined at w/c+f = 0.30. The reference PC_{sp} mortar had zero flow, but was fully compactible during molding; whereas the fly ash-containing mortar, PC–FA_{sp}, containing 58% fly ash and 42% Portland cement had a flow of 37 (compared with 100–110 required for ASTM C109 compliance). The reference PC_{sp} mortar reached 53.7 MPa (7,783 psi) after 28d and was significantly stronger than the ASTM C109 mortar at all ages (Fig. 1). By comparison, the PC–FA_{sp} mortar reached 38.2 MPa (5,538 psi) after 28d and had reached parity with the ASTM C109 mortar after only 14d, demonstrating the strength gain potential of the HVFA system at such high fly ash replacement levels. By 365d, the PC–FA_{sp} mortar had developed 62.9 MPa (9,125 psi), representing 143% of the ASTM C109 mortar strength at the same age.

Because of the differences in flow resulting from the use of a fixed w/(c+f) ratio, these strengths cannot be directly compared. Reduction of the water content of the PC–FA_{sp} mortar to obtain flow equal to that of the superplasticized PC_{sp} mortar would have substantially increased its strength. The feature of importance is the relative rate of strength development in the mortars (Fig. 1), from which it is clear that although the PC–FA_{sp} mortar lags behind the ASTM C109 mortar up to 14d and has only 70% of the strength of the PC_{sp} mortar at 28d, it continues to develop strength up to 365d.

3.3 Physical Microstructure of Pastes and Mortars

The development of microstructure in the HVFA systems is first examined in physical macroscopic terms by considering the morphology as determined by scanning electron microscopy and the pore structure based on the mercury intrusion porosimetry technique.

Morphology and Microchemical Features

The general morphology of fracture surfaces of the PC_{sp} and $PC–FA_{sp}$ pastes after 10h to 365d curing are shown in the accompanying scanning electron micrographs (Fig. 2).

10 hours: In the 10h pastes (Figs. 2a,b), the onset of hydration is clearly seen in both PC_{sp} and $PC–FA_{sp}$ systems, the predominant features being early ettringite deposition and the formation of amorphous-looking C–S–H. Deposition is more pronounced in the PC_{sp} pastes and is particularly heavy on the finer particles.

3 days: After 3d curing (Figs. 2c,d), cementation is quite advanced in both the PC_{sp} and $PC–FA_{sp}$ pastes. Both systems exhibit good intergrowth of binder phases into the pore space and bonding to particles. Where the reaction rims have fractured away in the $PC–FA_{sp}$ pastes (presumably a consequence of sample preparation), it is clear that the basic smooth morphology of the ash particles is preserved with no significant indications of 'etching' as a sign of chemical reactivity. There are no obvious morphological signs of the presence of calcium hydroxide at this age in either system.

28 days: The 28d pastes (Figs. 2e,f) show further densification as a result of extensive pore filling by the hydration products. There is also some indication in the $PC–FA_{sp}$ pastes that ettringite crystals, where they are observable, have a higher aspect ratio (i.e. longer and thinner) than the PC pastes. There are still no major morphological changes in the visible fly ash particles which might be associated with chemical reaction, although etch-pits are starting to form on some of the particles. Again, there are no obvious signs of calcium hydroxide precipitation.

90 and 365 days: By 90d (Figs. 2g,h) and extending to 365d (Fig. 2i,j), the gap-filling process continued in both systems, although there is some indication that the PC_{sp} paste is more fully densified than the $PC–FA_{sp}$ system. At these late curing ages, more advanced etching of many of the fly ash particles is observable in the $PC–FA_{sp}$ pastes, although the spherical shape clearly remains in sample at 365d.

Mortars: Scanning electron micrographs of fracture surfaces from a 28-day $PC–FA_{sp}$ mortar are shown in Figure 3. It can be seen that, with the obvious exception of the presence of sand grains, the overall morphology of the mortars is similar to the pastes. The matrix is well densified and there is good bonding between the binder and both the fly ash particles and the sand. For the former, bonding was apparently so good that fracture can be seen to occur through a fly ash particle (Fig. 3b). There is no obvious indication of the familiar deposition of calcium hydroxide at the interface between the sand grains and the

matrix. As is seen in the pastes, there are signs that chemical attack (etching) on the fly ash glass has commenced at 28d.

In summary, the pastes and mortars show good densification as a result of the pore-filling qualities of the hydration products. In the PC–FA_{sp} system, it is obvious, first, that the fly ash particles themselves are contributing significantly to space filling, and second, that the particles provide additional sites for the nucleation and growth of the binder phases. These are considered to be important physical aspects of the behaviour of HVFA materials. The binder particularly at later ages shows no distinct morphological features which allow it to be assigned as C–S–H type I, type II, etc. Other workers [17] have reported similar findings in low w/c ratio pastes where it is postulated that the comparative lack of pore space does not allow the characteristic C–S–H morphologies to develop in the same way as high w/c pastes. Of particular note is the fact that the familiar hexagonal plates of $Ca(OH)_2$ are not observed in the pastes at any age.

Pore Structure

From the mercury porosimetry data for the superplasticized PC_{sp} and PC–FA_{sp} pastes (Table 5, Figs. 4 and 5), it can be seen that both paste series showed the usual general decrease in total porosity with age, but at markedly different rates. Figure 13 summarizes the pore volume data for both paste systems, from which it is clear that the PC_{sp} pastes exhibit lower porosity than the PC–FA_{sp} pastes at corresponding ages. In both systems total porosity reached a minimum of ~21% at 28 to 56d; however, for the PC–FA_{sp} pastes, there is an apparent increase in total porosity at later ages. It is notable, however, that both series of superplasticized pastes exhibit porosities which are typically 60–70% of those for comparable pastes prepared at w/c = 0.5 with no superplasticizer.

Following the general approach of Roy and Parker [18], the pore size distributions of the pastes can be examined more closely by considering the maxima in the differential pore size plots (i.e. dV/dP vs. pore size). These plots (Fig. 4a,b) show a 'critical pore size' or the 'maximum continuous pore size,' which is considered to represent the largest fraction of interconnected pores in the sample and can be used as a measure of the rate at which the pore spaces in the paste are filling with cementitious hydrates. It can be seen that, as expected, the critical pore size in the PC_{sp} pastes decreased as the curing age advanced (i.e. from ~2 μm at 2–10h, to ~0.5 μm at 1d, to ~0.05 μm after 28d). Beyond 28d, there are uncertainties in the data as the detection limits of the instrument are approached (due to the very low porosity of the samples). After 7d, there appears to be two dV/dP maxima in the PC_{sp} pastes at ~0.1 and ~0.02 μm, which is a feature not previously observed in the data for unsuperplasticized PC pastes [3–5].

The corresponding data for the PC–FA_{sp} pastes are generally similar to the PC_{sp} pastes, the notable difference being the greater open porosity in the PC–FA_{sp} pastes than in the PC_{sp} pastes at comparable ages (note, however, that this is a relative statement and that the absolute porosities are very low for both systems). This is shown by both the peak

height/areas of the dv/dP plots (Fig. 4) and in the curves of cumulative pore volume vs. pore diameter (Fig. 5). It is of particular interest to note that, for the latter, the profiles of all the 90 and 365d distribution curves are continuing to rise below 0.05 μm (corresponding to the 60,000 psia limit of the porosimeter), suggesting that additional microporosity is present in the samples and beyond the range of the technique. This feature has been reported for other low w/c ratio pastes prepared with silica fume [19].

It is also noted that the double maxima in the dV/dP curves for the cement pastes appears to be absent in the fly ash pastes, although the ultimate continuous pore size (as detectable by this method) is similar at ~0.02 μm in both systems, appearing at ~7d for the PC_{sp} pastes and ~28d for the PC–FA_{sp} pastes. By way of comparison, it should also be noted that the maxima in the comparable unsuperplasticized pastes at w/c = 0.5 was observed at the much larger pore size of ~0.1 μm [3-5].

In summary, the present data indicate that there are subtle differences in the physical microstructure of the HVFA pastes when compared to the reference PC paste which are largely manifested in terms of relatively greater open porosity. A mechanism is indicated for the formation of porosity at late ages in the HVFA pastes. There is also some indication from the observation of the multiple dV/dP maxima that the pore structure of the two systems is different. Both systems, however, exhibit extremely low porosities which are at the limits of detection for the porosimetry technique.

It is important to note that additional microporosity is likely present for both series of superplasticized pastes beyond the detection range of the porosimetry technique. Whether the fly ash pastes have less of this microporosity than the PC pastes cannot be determined from the present data and remains to be addressed. If this is the case, it could explain the relative ease of fluid extraction from the PC–FA_{sp} pastes at ages up to 365d, while no pore fluid could be extracted from the PC_{sp} pastes beyond 7d curing (see Section 3.7). The fluid extraction property of the PC–FA_{sp} pastes is considered to be a significant characteristic of the HVFA materials and one which must be related in some way to the pore structure.

3.4 Solid Phase Identification in Hydrated Pastes

On the basis of the X-ray powder diffraction data recorded for the paste materials up to 365d (Figs. 6-8, Table 6), the following general observations can be made concerning the solid phases involved in the hydration reactions:

(i) During the period 2h to 3d, as the Portland cement hydrated, both the PC_{sp} and PC–FA_{sp} pastes showed a general decrease in alite (C_3S), belite (C_2S) and calcium sulphates (anhydrite and gypsum) with time and a corresponding increase in the levels of $Ca(OH)_2$ and ettringite (AF_t). Up to 365d, unambiguous features attributable to silicate hydration products

(e.g. C–S–H) were not observed, which implies that they likely have a low degree of crystallinity.

(ii) Unreacted C_3S and C_2S in both paste systems are observable in significant concentration even after 365d curing, indicating incomplete reaction of the Portland cement.

(iii) Although the present XRD data were not determined in a manner permitting quantitative interpretation, there are indications from peak height measurements that ettringite (AF_t) in PC–FA_{sp} samples is formed both at an earlier age (~5h), and in larger concentrations, than in the PC_{sp} control pastes. This is significant because the fly ash pastes contain only 42% of the PC present in the PC_{sp} control pastes. The implication is that the additional ettringite is somehow related to reactions involving the fly ash.

(iv) For the PC–FA_{sp} pastes, the ettringite peaks appear to be displaced to lower values of 2θ (larger d-spacing), suggesting that the ettringite may have some iron substituted for aluminum [20].

(v) A relative decline in $Ca(OH)_2$ content appears to have occurred in the fly ash pastes starting between 3 and 14d. While only qualitative, these data tend to support the conclusions drawn from the quantitative pore fluid and thermal analysis experiments discussed below.

(vi) Neither series of pastes show evidence for the formation of calcium monosulphoaluminate (AF_m) up to 365d curing.

(vii) There is some indication that the broad diffraction maximum at 20-25° 2θ produced by the fly ash glass decreased with curing age, suggesting chemical reaction of the ash.

More detailed examination of the XRD data is required, particularly to characterize the binder phases and quantify the above observations. The preliminary indications are that the hydration of the Portland cement in both superplasticized PC_{sp} and PC–FA_{sp} pastes is far from complete even after 365d curing. Also, the rate and extent of ettringite (AF_t) formation in the PC–FA_{sp} pastes are greater than in the PC_{sp} pastes. Coupled with the observed decline in the calcium hydroxide levels at longer curing ages, these observations point clearly to chemical involvement of the fly ash in the hydration of HVFA pastes.

3.5 Extent of Hydration: Calcium Hydroxide and Bound Water

The major components of a Portland cement paste in regard to late-age binder composition are the hydrates of alite (C_3S) and belite (C_2S). When C_3S and C_2S react with water, calcium silicate hydrates (commonly referred to as C–S–H gel) of poorly defined structure and stoichiometry are formed together with $Ca(OH)_2$ (calcium hydroxide or Portlandite):

$$C_3S + n\,H_2O \rightarrow C\text{–}S\text{–}H + x\,Ca(OH)_2$$

and,

$$C_2S + m\,H_2O \rightarrow C\text{–}S\text{–}H + y\,Ca(OH)_2$$

Even in pastes cured for extensive periods of time, these reactions often remain incomplete, with unhydrated C_3S and C_2S grains being found in the pastes (this was noted for the low w/c pastes in the present study in the previous section). Further, because of the non-stoichiometric nature of C–S–H, the exact amount of $Ca(OH)_2$ produced on hydration is always uncertain. In general, it is common practice to assume that a fully hydrated Portland cement, with typical C_3S and C_2S content, will bind ~25-28% H_2O by mass with the production of ~20–25% $Ca(OH)_2$.

To obtain a quantitative estimate of the extent of hydration in pastes, methods based upon thermal analysis have been used by the authors in this and earlier studies [3-7,9]. Two parameters are of interest in the pastes as a function of curing age:

- the concentration of $Ca(OH)_2$
- the amount of 'bound' (non-evaporable) water

In comparing the extent of hydration in pastes of Portland cement with those comprising both Portland cement and a supplementary cementing material (SCM), three conditions are possible:

(i) All hydration results from reactions involving Portland cement only.

(ii) Hydration of Portland cement is either retarded or accelerated by the presence of the SCM.

(iii) Reactions occur that involve the formation of hydrates from constituents of the SCM, in addition to those from the Portland cement.

To test these possibilities, it is useful to examine the thermal analysis data in terms of both the concentration of $Ca(OH)_2$ and the level of bound water by relating these factors to the quantity of Portland cement in the original paste. Consideration of the data in this form (Table 7 and Fig. 14) shows the following features:

PC_{sp} pastes:

- The total production of $Ca(OH)_2$ (17.2%) up to 365d is considerably less than is normal for Portland cement.
- Similarly, the level of bound water (19.8%) at 365d is significantly lower than normal for a fully cured Portland cement.

PC–FA_{sp} pastes:

- In terms of $Ca(OH)_2$ production, the early hydration (from 2h to 1d) appears similar to the PC_{sp} paste, with minor retardation of hydration indicated at 10h.
- By 3d, the production of $Ca(OH)_2$ was higher than the PC_{sp} paste reaching a poorly defined maximum value in the range from 20.5% at 7d to 21.2% at 56d.
- A decline in $Ca(OH)_2$ content occurred in the PC–FA_{sp} pastes after 56d.
- When the data are normalized to the PC content of the pastes, extremely abnormal quantities of bound water were found in the PC-FA_{sp} pastes at ages later than 7d rising to a maximum of 54.87% at 56d.
- Curing beyond 56d resulted in a reduction in bound water to 30.2% by 365d.
- After 28d, and particularly at 90 and 365d, the DTG curves (Fig. 8) all show a rising profile at 1000°C (the high temperature limit of the Dupont 951 instrument), indicative of further mass loss potential at higher temperatures.

These data are taken to indicate the following:

(i) The PC_{sp} pastes do not fully hydrate, even on curing up to 365d.

(ii) At ages from 1d to 56d increased production of calcium hydroxide was observed in the PC–FA_{sp} pastes compared to the PC_{sp} pastes. The likely rationale for this observation is either that the fly ash has accelerated the hydration of the PC in the HVFA system, or that the higher effective w/c ratio in the fly ash system has favoured cement hydration.

(iii) A steady decline in calcium hydroxide content at late ages in the PC–FA_{sp} pastes may have resulted from pozzolanic reaction.

(iv) The exceptionally high levels of bound water, relative to the cement content, at late curing ages in the PC–FA_{sp} pastes indicate extensive participation of the fly ash in a hydrate phase. This is further supported by the rising DTG profiles at 1000°C in the long term pastes, which indicate that even more water may be bound in the structure, for example, in a silanol (Si–OH) form (as in silica gels).

Of these, observation (iv) is the most important. A level of bound water of 54.9% at 56d cannot be the result of hydration of the Portland cement only, and points to chemical reactivity of the fly ash in the HVFA system. This important point is discussed further below in Section 3.7.

3.6 Pore Fluid Chemistry and Paste Hydration: Theory

Before discussing the pore fluid composition data obtained during this study, it is necessary to consider some basic concepts of the chemical relationships in aqueous solutions containing Ca^{2+}, OH^-, SO_4^{2-}, Na^+ and K^+ ions. It is the relationships between these elements in the form of ions in solution that can be used to infer changes in the nature of the solid phases during hydration. Three factors need to be considered:

- The origin of each component, and the reactions in which they are involved during hydration.
- Changes in solution composition resulting from redistribution of water or other components from the solution to a solid phase.
- The thermodynamic state of the chemical components in solution in relation to ionic activity and the formation of complex or associated ion species.

The Origin of Ionic Species in Pore Fluids

Calcium in pore solutions originates at early ages from the dissolution of some of the calcium sulphate (usually gypsum and/or anhydrite) and calcium oxide in the Portland cement, and at later ages from hydration of the principal cementing phases (C_3S, C_2S). Both fly ash and Portland cement clinker contain sodium and potassium in various states of combination. In the present study, in addition to the sodium and potassium contributed by the cementing phases, consideration must also be given to the alkali content of the superplasticizer.

The principal source of sulphate in normal Portland cement systems is from the calcium, sodium and potassium sulphates contained in the cement. The sulphur content of Portland cement used in this study is 3.0% expressed as SO_3 and was present in the form of anhydrite ($CaSO_4$) and gypsum ($CaSO_4 \cdot 2H_2O$). The fly ash contained 1.3% SO_3, and also has the potential to contribute some sulphate to the PC–FA system. The superplasticizer was found on analysis to contain 15,500 mg/L of free sulphate and, therefore, can be expected to contribute considerably to the sulphate loading of the pastes.

Most of the hydroxyl ion in pore fluids results from the reaction between $Ca(OH)_2$ and sulphate ions to produce insoluble calcium sulphates. Some hydroxyl may come also from the hydrolysis of free CaO, Na_2O and K_2O in the Portland cement. The most soluble components in the system are the alkali metal sulphates (Na_2SO_4, K_2SO_4). In the absence of $Ca(OH)_2$, these form concentrated solutions of near neutral pH in water. However,

when $Ca(OH)_2$ is present, alkali sulphates will react to form gypsum, during the precipitation of which OH^-, Na^+ and K^+ ions enter solution, accompanied by a corresponding increase in pH in the pore fluid:

$$Ca(OH)_2 + M_2SO_4 = CaSO_4 \cdot 2H_2O + 2M^+ + 2OH^- \quad (1)$$

(where M = Na and/or K)

As a result, the overall balance of ions in the pore fluids is controlled by the quantity M_2SO_4 available and the solubility product relationships for $Ca(OH)_2$ and $CaSO_4 \cdot 2H_2O$, the condition of electroneutrality being expressed in terms of ionic concentrations, as follows:

$$\Sigma (2Ca^{2+} + Na^+ + K^+) = \Sigma (2SO_4^{2-} + OH^-)$$

Because both $Ca(OH)_2$ and $CaSO_4 \cdot 2H_2O$ are relatively insoluble, the concentrations of Na^+, K^+, SO_4^{2-} and OH^- in pore solutions are relatively high, and Ca^{2+} concentrations are low (normally 3–5 mmol/L) under equilibrium conditions.

In addition to the dissolution of $Ca(OH)_2$ and $CaSO_4 \cdot 2H_2O$ and the reactions resulting from the precipitation of gypsum, aluminate ions become available as hydration continues through hydrolysis of C_3A (after a short induction period). In the presence of Ca^{2+}, OH^- and SO_4^{2-}, the sulphoaluminate ettringite ($C_3A \cdot 3CS \cdot 32H_2O$) is formed by two reactions:

$$3CaSO_4 + 3Ca(OH)_2 + 2Al(OH)_3 = C_3A \cdot 3CS \cdot 32H_2O \quad (2)$$

The calcium sulphate for this reaction is available from both the Portland cement and by reaction (1). The complex salt ettringite is extremely insoluble and causes the pore water to become sub-saturated relative to $CaSO_4 \cdot 2H_2O$. The onset of the precipitation of ettringite is indicated by reduction in the Ca^{2+} and SO_4^{2-} ion concentrations in solution.

Changes in Solution Composition During Hydration

The chemical composition of pore solutions is determined by two factors. First, as was discussed above, the ions that enter solution come from the dissolution and precipitation of various solid phases, and to that extent composition is governed by the solubility of these phases. Secondly, the concentration of the components in solution is strongly influenced by the process of hydration during which water is removed from the pores to become a part of the solid structure.

In pore water extraction experiments, the hydration of cement paste is conducted in a 'closed system' — i.e. cement (or cement and fly ash) and water are mixed in a fixed ratio (w/(c+f) = 0.30) and the pastes are stored in sealed containers. Thus, as hydration proceeds, some of the water is removed from the liquid phase to the solid phase, thereby reducing the volume of free pore water. Additional water does not enter or leave the

system, as may be the case in a standard mortar or concrete system cured in contact with an external source of water.

Sodium and potassium ions can enter the pore water solution at any time during the experiment without the precipitation of a solid phase, both Na and K hydroxides and sulphates being strongly soluble. Therefore, unless other mass transport processes intervene, the concentration of these ions will increase with time as the total mass of liquid water is reduced by the formation of hydrated solids (analogous to the isothermal evaporation of a solution of a soluble salt). Consequently, changes in Na^+ and K^+ ion concentrations during hydration may be considered in terms of the volume (or mass) of solution present in addition to their solution concentration. Using an approach originally described by Diamond [21], the measured concentrations of Na^+ and K^+ ions in the pore solutions can be related to the original quantities of cement and water in the unhydrated pastes and can be used to detect net transport of alkalis between solution and solid phases during hydration.

Conversely, once relevant equilibrium saturation conditions have been reached in the paste, the concentration of Ca^{2+}, OH^- and SO_4^{2-} ions are constrained by the presence of solid lime, gypsum and ettringite phases. Thus, as the volume of liquid water decreases, insoluble compounds will precipitate and leave the solution phase saturated with respect to these salts. Unless major changes occur in ionic strength or ion-pair formation, changes observed in Ca^{2+}, OH^- or SO_4^{2-} concentrations during hydration may be taken to indicate their participation in chemical reactions and/or phase transitions.

Thermodynamic Relationships in Pore Fluids

In studying the microstructure of hydrating cement systems, the purpose of investigating the composition of pore fluids is to detect the formation or disappearance of solid phases during hydration. To achieve this, it is necessary to know at any particular stage of curing whether the relevant solubility of the solid phase of interest has been exceeded. At equilibrium, a solid phase will precipitate only if the solution is saturated with respect to the ions comprising that phase. The status of the solution is conveniently expressed in terms of an ionic product, such as:

$$[Ca][SO_4]$$

At saturation, the ionic product reaches a constant value termed the solubility product (K_{SP}). Ionic products in excess of this value characterize solutions that are super-saturated with respect to the phase under consideration.

Because the solubility of a solid and the associated phase changes that accompany solution are governed by the chemical potential or free energy change of the system, considerations of gross chemical composition are not appropriate to the calculation of solubility products in concentrated solutions. The thermodynamic solubility product required to detect the degree of saturation of a solution must be calculated in terms of ionic activity. Chemical

analysis of pore water solutions determines the total chemical composition, without regard to the state of aggregation of solution components. To determine ionic activity, consideration must be given to the concentration of ions, relevant activity coefficients, and the potential formation of complex ions and ion pairs in solution.

In other research [22], the present authors have developed a theoretical approach that permits the ionic status of pore fluid solutions to be calculated in thermodynamic terms. This approach draws on some earlier work published by Bailey and Hampson [23]. The computation allows for the presence of simple ions (e.g. Ca^{2+}, Na^{+}, K^{+}, SO_4^{-}, and OH^{-}) and the formation of ion pairs, e.g. $(CaOH)^{+}$, $(CaSO_4)^{o}$, $(NaSO_4)^{-}$ and $(KSO_4)^{-}$. This approach, the details of which will be published elsewhere, has been applied to interpret the pore solution data from the present study to provide a basis for a consideration of reactions occurring during hydration of the pastes.

3.7 Pore Fluid Chemistry and Paste Hydration: Mechanistic Implications

The experimental data obtained from this study are now examined in terms of possible mechanisms relating the developing solid phases and the pore fluid compositions in the HVFA systems at different hydration ages.

Pore Fluid Composition

Because the Portland cement, the fly ash and the superplasticizer all contribute Na, K and SO_4 to the pastes, it is valuable, as a first step, to know the total concentration of each of these species in the original mixtures. The calculated quantities of these species in the paste raw materials (expressed as mmol/L of the original volume of mix water) are given in Table 9 and can be compared with those from the chemical analyses of the pore fluids extracted from the pastes (Table 8). Figure 12 shows a graphical representation of the variation in Ca^{2+}, Na^{+}, K^{+}, Si^{4+}, SO_4^{2-} and OH^{-} concentrations in the reference PC_{sp} pastes up to 7d of curing, in comparison with corresponding data for the PC–FA_{sp} pastes to 365d. It should be noted that pore fluids could only be extracted in any measurable amount from the PC_{sp} pastes at ages up to 7d. In contrast, it was possible to extract pore fluids from the PC–FA_{sp} pastes at all ages up to 365d. Observations from these data may be summarized as follows:

(i) Portland cement (PC_{sp}) pastes showed exceptionally high levels of calcium (34.9 mmol/L) at 2h, in comparison to the levels normally expected from Portland cement systems (typically 3–5 mmol/L). Similar, but less markedly high Ca concentrations were found for the PC–FA_{sp} pastes at 2h and 5h.

(ii) Minima in the concentration of Ca in solution from both paste systems were observed at 10h for the PC_{sp} paste and at 1d for the PC–FA_{sp} paste.

(iii) Sodium, potassium and hydroxyl concentrations were unusually high in all of the solutions.

(iv) In the PC–FA_{sp} paste, sodium and to a lesser extent potassium concentrations showed maxima at 7 and 28d, respectively.

(v) Silicon and to a lesser extent aluminum were found in solution at higher than normal levels in both sets of pastes. The elevated concentration of silicon being higher and occurring at an earlier age for the PC_{sp} paste.

(vi) The marked fall in sulphate concentration usually attributed to ettringite formation was found to occur in both pastes after 1d

When the alkali ion concentrations are calculated relative to the initial paste composition (Table 10 and Fig. 15), it is evident that transfer of sodium from solution to the solid state occurred in the PC–FA_{sp} pastes all at ages in excess of 3d. Evidence of transfer of potassium is less certain. There is no evidence of similar transfer of alkali ions in the PC_{sp} pastes up to 7d (the maximum age at which pore solutions could be expressed from the PC_{sp} system). The apparent mass transfer of alkalies to a solid component is considered indicative of reactions involving fly ash glasses (see below). Beyond these observations, there is little that can be established by consideration of the raw analytical data. In order to interpret the observations, consideration must be given to the calculated ionic status of the solutions, as discussed below.

Calculation of Aqueous Phase Compositions

Tables 11 and 12 present a summary of the principal parameters describing the thermodynamic conditions of pore fluids from PC_{sp} and PC–FA_{sp} pastes as a function of curing age. To aid interpretation of these data, saturation factors relative to $Ca(OH)_2$ and $CaSO_4 \cdot 2H_2O$ have been calculated (Figs. 16 and 17). Uncertainties as to the composition and the solubility product of AF_t phases preclude a similar treatment for this compound. The following general observations are made:

(i) The ionic strength of pore fluids is seen to range from 0.22 to 0.65 molar. These are sufficiently high that it is appropriate to consider ionic *activities* rather than concentrations. Under these conditions, activity coefficients of some ions (notably Ca^{2+} and SO_4^{2-}) may be as low as 0.3 to 0.5.

(ii) Hydroxyl ion concentrations are exceptionally high, reaching >1.0 molar in PC_{sp} pastes. Thus, it is necessary to consider the potential formation of the ion-pair $(CaOH)^+$ as a significant factor in maintaining calcium in solution. Similar considerations should also be given to three sulphate-containing ion-pairs: $(CaSO_4)^o$, $(NaSO_4)^-$ and $(KSO_4)^-$ in solutions of high sulphate content.

(iii) In the pore solutions from PC_{sp} pastes during two curing periods (from 2–5h and >10h), conditions of extreme supersaturation relative to $Ca(OH)_2$ persisted. Supersaturation to $CaSO_4 \cdot 2H_2O$ was observed only at 2h.

(iv) In the pore solutions from $PC–FA_{sp}$ pastes, supersaturation relative to $CaSO_4 \cdot 2H_2O$ was observed up to ~10h. Some supersaturation relative to $Ca(OH)_2$ was found after ~3d, but it was minor in comparison with that for the PC_{sp} pastes.

(v) Most notable is the observation that, while the $PC–FA_{sp}$ pastes were sub-saturated to $CaSO_4 \cdot 2H_2O$ by some two-orders of magnitude at all ages after 10h, the PC_{sp} pastes did not reach levels of sub-saturation lower than SF≈0.26 up to 7d.

These observations are considered below in terms of three mechanistic factors:

- early age supersaturation
- the formation of gypsum ($CaSO_4 \cdot 2H_2O$) and ettringite (AF_t) phases
- late-age supersaturation

Early Age Supersaturation

Pore fluids extracted at 2h from the superplasticized PC paste were strongly supersaturated relative to both $Ca(OH)_2$ and $CaSO_4 \cdot 2H_2O$ (SF≈28). A minor degree of supersaturation (SF≈2-4) to gypsum is not unusual in cement systems at very early ages (15 min to lh) and has been attributed [23] to the dissolution of anhydrite ($CaSO_4$) or calcium sulphate hemihydrate ($CaSO_4 \cdot 0.5H_2O$). However, supersaturation at the observed levels must have resulted from some other cause.

The total concentrations of calcium, sulphate and hydroxyl in the pore solutions from the PC_{sp} pastes (Table 8) during the period up to 10h were as follows:

Age	Ca (mmol/L)	SO_4 (mmol/L)	OH (mmol/L)
2h	35	242	209
5h	3	254	200
10h	0.5	254	266

It must be concluded from these data that the cause of supersaturation is the presence in solution of large quantities of calcium. A likely cause of this is the formation of complex ions in solution, the most probable being a complex formed with a component of the superplasticizer, for example:

$$[Ca \ldots N\text{-F.sulphonate}]^{n+}$$

The level of supersaturation (SF≈4.6–4.8) observed relative to $CaSO_4 \cdot 2H_2O$ in the fly ash-containing PC–FA_{sp} pastes is less strongly indicative of complex ion formation, although it is higher than normal.

Although the possibility of complex ion formation in the PC_{sp} paste is not of concern in relation to the binding reactions in PC–FA_{sp} pastes, it is of considerable interest in relation to the general behaviour of superplasticizers in cement systems.

Because the system was so supersaturated up to 5h, and because we have no knowledge of the stability constants for any complex ions formed, we cannot use the pore solution data to infer solid phase conditions at ages less than 2h.

Formation of Ettringite and Gypsum

During the period 5–10h, four processes appear to have dominated the pore solution conditions of both pastes:

$$Ca(OH)_2 \rightarrow Ca^{2+} + 2OH^- \quad (3)$$

$$CaSO_4 \cdot 2H_2O \rightarrow Ca^{2+} + SO_4^{2-} \quad (4)$$

$$M_2SO_4 + Ca(OH)_2 \rightarrow CaSO_4 \cdot 2H_2O + M^+ + OH^- \quad (5)$$

$$3Ca(OH)_2 + 3CaSO_4 + 2Al(OH)_3 \rightarrow C_3A \cdot 3C\bar{S} \cdot 32H_2O \quad (6)$$

As a consequence, while the solutions declined from supersaturation to sub-saturation with respect to lime and gypsum, the quantities of alkali, sulphate and hydroxyl in the solution phase remained relatively constant (Table 13). Examination of the corresponding solid phases showed ettringite to be present at ages >2h; no gypsum was detected and calcium hydroxide was detected at low concentrations (higher in the PC_{sp} system). The formation of ettringite (eqn. 6) appears to have progressed at a sufficient rate to consume the gypsum form the original cement and that produced from alkali sulphates (eqn. 5).

By 1d, sulphate in the pore solution declined in both pastes with a corresponding increase in OH. The decline in sulphate in solution indicates the completion of ettringite formation from initially soluble components. XRD results indicate that in both systems ettringite precipitation was essentially complete by 1d. However, the quantity of ettringite in the pastes remained constant through 365d, with an indication by XRD that more was precipitated in the PC–FA_{sp} paste than with Portland cement alone.

From the appearance of ettringite in the XRD and TGA, and the expected behaviour of Portland cements, it is reasonable to assume that tricalcium aluminate (C_3A) hydration in the pastes had been initiated by 2–5h. As a result, the phase system $CaO–Al_2O_3–CaSO_4–H_2O$ is relevant to the solution conditions. This phase system (Fig. 18) has six invariant points:

B	CH, $C\bar{S}$
D	AH_3, C_3AH_6
E	AH_3, Et, $C\bar{S}$
H	AH_3, Et, C_3AH_6
F	CH, Et, $C\bar{S}$
G	CH, Et, C_3AH_6

Of these, invariant point **D** is relevant only at conditions of low SO_4 concentration and low pH; invariant point **B** is relevant only to the lime/gypsum system; and invariant points **E** and **H** do not include $Ca(OH)_2$ as an equilibrium phase. Because the hydration of C_3A is the source of alumina, the hydrate C_3AH_6 is likely present. Consequently, the most likely phases in equilibrium with the pore fluids are represented either by invariant point **G** (CH, Et, C_3AH_6) or point **H** (AH_3 , Et, C_3AH_6)

In the case of the reference PC_{sp} pastes during the period 2–10h, no significant changes in the mass of Na, K, SO_4 or OH occurred in solution (Table 10). This is taken to imply that any soluble alkali sulphates in the PC_{sp} pastes had all entered solution by 2h, and that the reactions between them and lime to produce calcium sulphate:

$$M_2SO_4 + Ca(OH)_2 = CaSO_4{\cdot}2H_2O + 2M^+ + 2OH^-$$

were completed by 5 hours.

Overall, the solution conditions at 5 to 10 hours are consistent with the formation of ettringite from calcium sulphate and lime:

$$3Ca(OH)_2 + 2Al(OH)_3 + 3CaSO_4 = C_3A{\cdot}3C\bar{S}{\cdot}32H_2O$$

In the fly ash-containing pastes, the following observations are relevant:

(i) $Ca(OH)_2$ was found only in trace quantities by TGA at ages <1d.

(ii) Potassium quantities increased markedly in the pore solutions during the period from 5 to 10 hours of hydration.

These factors indicate that in the fly ash system, reactions involving alkali metal sulphates were more active in producing calcium sulphate than for the PC_{sp} pastes. It is tentatively proposed that in the fly ash system the equilibrium solid phases are likely to be AH_3, Et, and C_3AH_6 (Point **H**), although the level of AH_3 is probably low due to its consumption in the formation of ettringite and the relatively slow rate of C_3AH_6 formation from C_3A. This is consistent with the lower overall content of lime in a system that contains 58% fly ash.

To summarize, there is some indication that the mechanism of sulphoaluminate formation is different for the two paste types. Ettringite being formed in the fly ash pastes largely by

reactions involving alkali sulphates, presumed to originate in the fly ash, rather than by consumption of gypsum and or anhydrite.

Late Age Supersaturation

In the PC_{sp} pastes, by 1d and through to 7d (no data being available beyond this age), extreme supersaturation to $Ca(OH)_2$ coexisted with minor sub-saturation to $CaSO_4 \cdot 2H_2O$. However, during this period, both TGA and XRD analysis (Tables 6 and 7) showed the presence of $Ca(OH)_2$ (up to 8.5% by TGA). The presence of $Ca(OH)_2$ in such quantities is only consistent with supersaturation if the system is subjected to an influx of hydroxyl ions. The most likely source of hydroxyl ions in this case is the superplasticizer.

The superplasticizer (Table 2) is described as a sodium salt of a sulphonated naphthalene formaldehyde (N–F) condensate with the following simplified form:

$$[(N\text{–}F)SO_3]^- \; Na^+$$

Depending upon the 'acid-strength' of the $[(N\text{–}F)SO_3]^-$ group, this compound may produce an acid, basic or neutral reaction in water. In practice, most salts of this type are weakly basic and produce solutions of pH > 7.0. For simplicity of discussion, it has been assumed that the system is neutral, such that:

$$(N\text{–}F)SO_3\,M \xrightarrow{H_2O} (N\text{–}F)SO_3^- + M^+$$

If the organo-sulphonate ion $[(N\text{-}F)SO_3^-]$ is removed from solution — for example by precipitation of a calcium salt — the consequent ionic charge imbalance will be accommodated by formation of hydroxyl ions:

$$2(N\text{-}F)SO_3\,M + 2Ca(OH)_2 \rightarrow Ca[(N\text{-}F)SO_3] + 2M^+ + 2OH^-$$

A similar process would occur if the $[(N\text{-}F)SO_3]^-$ group were chemically adsorbed at a hydroxylated surface site:

$$\boxed{surface}\text{–}OH + (N\text{-}F)SO_3^- \rightarrow \boxed{surface}\text{–}SO_3(N\text{-}F) + OH^-$$

In both cases, the aqueous phase would become enriched in hydroxyl ions and, if the level of calcium in solution was low due to other processes (e.g. ettringite precipitation), apparent supersaturation relative to $Ca(OH)_2$ would result.

In summary, the extensive supersaturation of the pore fluids from the PC_{sp} pastes after 1d is attributed to immobilization of the organo-sulphonate component of the superplasticizer by either precipitation as a calcium salt or by chemisorption at hydroxyl sites on cement particles.

This supersaturation was not observed in the PC–FA_{sp} pastes until 365d and was not accompanied by a major influx of hydroxyl ions. A mechanism appears to exist, in the PC–FA_{sp} system, whereby the OH^- concentration and the quantity of Na and K in solution (Table 10) both decrease with age, while pore fluids remain saturated to calcium hydroxide and ettringite. Evidence from the examination of the extent of hydration (see Section 3.4) indicates that this may be achieved by reaction of the fly ash particles with M^+ and OH^- ions.

3.8 Fly Ash Hydration

From the discussion in the previous sections, it can be seen that there is considerable evidence that the fly ash must be participating chemically as well as physically in the HVFA materials, as follows:

- the significant strength development beyond 90d
- etching of fly ash particles observed in the SEM
- acceleration of cement hydration
- high levels of bound water
- reduced calcium hydroxide at late ages
- increased levels of ettringite (AF_t) at all ages
- markedly different solution chemistry in terms Na, K and OH quantities in solution at different curing ages (Table 10).

These observations point to chemical involvement of the Lingan fly ash in the short-term sulphoaluminate reactions as well as longer-term aluminosilicate hydration (i.e. pozzolanic hydration reactions). Although the details of these reactions are still unclear, the following working model is proposed as a basis for further investigation of HVFA materials.

Short Term (Sulphoaluminate) Reactions

Fly ash is a source of both sulphate and 'alumina' for the formation of sulphoaluminates, in addition to those derived from the Portland cement. It is difficult to be certain of the speciation of the sulphur. Some may be associated with alkali sulphates (M_2SO_4, $M'SO_4$, where M = Na, K; M' = Ca) deposited on the surface of the particles in the boiler flame; but the bulk is likely intimately associated with the surface aluminosilicate glass as dissolved SO_2/SO_3. The 'alumina' is a major constituent of the aluminosilicate glass, which for the Lingan fly ash has been shown [24] to have the following approximate composition ranges for different particles: SiO_2 44–59, Al_2O_3 8–30, Fe_2O_3 8–25, CaO 0.6–4.4, MgO 1.3–1.9, Na_2O 0.5–1.0, K_2O 2.1–6.3%. This glass-bound 'alumina' should not be confused with the total analytical Al_2O_3 which necessarily also contains a major contribution from the aluminum in mullite ($3Al_2O_3{\cdot}2SiO_2$), which is essentially inert in a cement system.

The surface-deposited sulphate will be available immediately to the system, whereas the availability of the glass-associated alumina and sulphate will depend on the rate at which the surface glass is attacked by alkali (see below):

$$\underset{\text{(aluminosilicate)}}{\equiv Si{-}O{-}Al\equiv} + M^+OH^- \rightarrow \equiv Si{-}OH + \underset{\text{(aluminate)}}{[Al(OH)_4]^-M^+}$$

In the presence of calcium and sulphate ions at high pH, the fly ash-derived aluminate can be expected to react rapidly to form ettringite:

$$2[Al(OH)_4]^-M^+ + 3Ca(OH)_2 + 3CaSO_4 \rightarrow C_3A{\cdot}3C\bar{S}{\cdot}32H_2O + 2M^+$$

In the absence of sufficient sulphate, calcium aluminate hydrates could also form:

$$[Al(OH)_4]^-M^+ + nCa(OH)_2 \rightarrow C_4AH_{13}, C_3AH_6, \text{etc.} + M^+$$

The tendency for ettringite to be strongly associated with the surface of the fly ash spheres has been noted in this and other studies of Portland cement–fly ash systems by the authors [3-5,25]. It is now proposed that this ettringite is one product of the hydration of the fly ash and is an indication that the aluminosilicate glass is being attacked. The ettringite may contribute significantly to early strength in the HVFA system.

In the short term, as aluminum is being leached from the glass, the overall matrix structure is maintained by the silica skeleton, and it is likely that there will be little perceivable change in the appearance of the fly ash particles. This effect has been observed by the authors [26,27] in studies of acid-leached fly ash. Products of reactions such as those proposed above, where the original form of a solid remains unaltered after extensive chemical modification are termed "pseudomorphs." This same term might aptly describe fly ash in cement systems in the early phase of curing, the resulting fly ash particles being termed "pseudomorphic" spheres.

Long Term (Pozzolanic) Reactions

As reviewed recently by the authors [28,29], the major and principal reactive component of fly ash is the aluminosilicate glass, which for the Lingan source has been shown [3-5] to comprise ~58% by mass of the material (the remainder being quartz, mullite, spinel and hematite, all of which can be considered to be unreactive in a cement system). The principal elements in the Lingan fly ash glass are Si, Al and Fe with smaller quantities of the glass modifier elements Na, K and Ca. It is these elements which are supplied by the fly ash and which have the potential to modify the cementing system.

The glass can be considered to be a disordered three-dimensional Si–O–Si network with aluminum (and some iron) substituting for approximately one-third of the silicon atoms. In the strongly alkaline media of the pore fluid (pH > 13.5), the aluminosilicate network will

be depolymerized by bond breaking at the siloxane (Si–O–Si) and silaloxane (Si–O–Al) linkages:

$$\equiv Si{-}O{-}Si\equiv + M^+ OH^- \rightarrow \equiv Si{-}OH + \equiv Si{-}O^- M^+$$
$$(M = Na \text{ or } K)$$

This process may be considered as a combination of hydrolysis and alkali sorption or ion-exchange. Such a mechanism offers an explanation for two features observed in this study:

- The transport of alkali from solution to solid phases at ages >7d in the PC-FA_{sp} system (see Table 10 and Fig. 15).
- The high level of bound water, in the hydrated glass, this being in the form of silanol groups that condense on heating during the TGA experiment:

$$\equiv Si{-}OH + HO{-}Si\equiv \rightarrow \equiv Si{-}O{-}Si\equiv + H_2O$$

In these reactions, the silicon is a centre for nucleophilic attack by the hydroxyl (OH^-) and the result is silanolation of the glass. Because silanol groups are weak acids, exchange of a proton with a Na^+ or K^+ ion is favoured. The rate of these reactions will be controlled largely by the diffusion of ions through the glass (a slow process). As the reaction proceeds, the surface of the glass will be depleted first of aluminum (see above) and will be extensively silanolated though at the same time retaining its physical form. Eventually, the outer silicate units will have depolymerized sufficiently for them to enter solution as soluble silicate, at which point they will react further with calcium ions to form insoluble calcium silicate hydrates:

$$[SiO(OH)_3]^- + Ca(OH)_2 \rightarrow C{-}S{-}H$$

A second mechanism is possible, based on ion-exchange reactions involving Ca^{2+}, M^+ and $\equiv Si{-}OH$ groups bound to the solid glass surface:

$$\equiv Si{-}OH + Ca^{2+} + 2OH^- \rightarrow \equiv Si{-}O\,Ca + H_2O$$

$$\equiv Si{-}O\,M + 0.5\,Ca^{2+} + OH^- \rightarrow \equiv Si{-}O\,Ca_{0.5} + MOH$$

Reactions of these types would explain both the decrease in bound water and the reappearance of M^+ and OH^- in solution at ages >56d.

As the outer regions of the glass shell are attacked, more internal surfaces are exposed and the process repeats itself. The C–S–H formed from the fly ash will supplement that formed from the cement and will serve as additional binder. This is the essence of the so-called pozzolanic reaction. Since the diffusion of ions through the glass is slow and the most likely rate determining step, the pozzolanic reaction is necessarily slow. This mechanism is consistent with the characteristically long induction period for pozzolanic cements in

general, and in the present case, the excellent long-term strength development in the HVFA systems.

At this stage, it is not clear how far aluminum or iron might be included in the pozzolanic reactions in the HVFA materials. In the absence of sufficient sulphate to form ettringite, it is possible that silicoaluminate hydrates, such as gehlenite hydrate (C_2ASH_8), could also be formed, as reported by Verhasselt [30]:

$$AS_2 + 3CH + z\,H \rightarrow C\text{–}S\text{–}H_{z-.5} + C_2ASH_8$$

This is supported by the work of Sersale and Orsini [31] who reported that C–S–H and C_2ASH_8 are formed in lime–pozzolan pastes, and that C_4AH_x and the solid solution with end members C_3AS_3 – C_3AH_6 (garnet – hydrogarnet) are also formed under certain conditions. The formation of gehlenite hydrate, however, is not predicted by a study carried out by Dron [32,33] of the $CaO–Al_2O_3–SiO_2–H_2O$ phase equilibrium system (Fig. 19) which indicates that C_2ASH_8 cannot coexist with $Ca(OH)_2$. It should be noted, however, that Dron's conclusions are based on strictly equilibrium conditions which, as other workers have noted [34], are unlikely to be present in a complex, multi-phase hydrating cement–fly ash system. Other studies by Sersale [35] and Masazza [36] point to the possible formation of both calcium aluminate hydrates and hydrogarnet in Portland cement–fly ash mixtures.

In summary, while ettringite (AF_t) is considered to be a product of the early hydration of the fly ash, it is not clear from the available data exactly what other hydration products are formed in the long term reactions (up to 365d). On the basis of the high levels of bound water, it is proposed that hydration (silanolation) of the fly ash glass is occurring in the highly alkaline pore fluid. Such a mechanism can be extended to explain the apparent transport of OH, Na, and K in and out of the pore fluid system (see above) and the high bound water content. Subsequent reaction between Ca^{2+} and the Si–OH rich gel or Si–OM (M = Na, K) species released into solution (by further depolymerization of the silanolated glass) would be expected to lead to the formation of additional C–S–H, either at the surface of, or remote from, the fly ash particle, respectively. A preliminary model for the sequence of reactions involved in the attack on the fly ash glass is shown in Figure 20.

The fate of the iron in the Lingan ash in these reactions is not at all clear from the available data, although there is some evidence from the XRD data that it might be incorporated in the AF_t phases. The possibility of precipitation of hydroxylated iron species cannot be discounted in the system. The scope of present study did not extend to investigation of this issue though such work is warranted.

The observation of high bound water contents with little depletion in calcium hydroxide content after long curing ages (~1 year) was recently reported by Diamond [37] for other fly ash pastes not containing superplasticizer. It may be a general phenomenon in fly ash Portland cement systems and an investigation of this process is required.

4. CONCLUSIONS

The following conclusions have been drawn from the present examination of the HVFA pastes and mortars (no order of importance is implied):

1. The HVFA mortars (58% fly ash, w/c = 0.715) exhibit excellent long-term strength development beyond 90d curing, at which point they comfortably exceed (relative strength 124%) the performance of a reference ASTM C109 Portland cement mortar (w/c = 0.464). This characteristic can only be associated with pozzolanic reaction of the fly ash.

2. Physically, it is clear that the high levels of fly ash efficiently fill space in the matrix while acting as additional centres for the growth of cementitious hydrates. This behaviour, in addition to the reduced w/c+f ratio induced by the use of superplasticizer, provides increased densification of the developing matrix. It is also possible that the fine particle effect of the fly ash spheres acts to alter the initial floc structure of the hydrating cement.

3. The HVFA pastes have low porosity (~22-30%) and a very fine pore structure which appears to be more open than the reference superplasticized PC paste. There is evidence for microporosity below 0.02 μm. Related to the differences in pore structure, is the observation that pore fluid can be extracted from the HVFA pastes up to 365d, whereas this was only possible in the PC pastes up to 7d.

4. Although the cement in the HVFA pastes was not fully hydrated, even at 365d, there is evidence that, after an initial retardation period up to ~1d, the hydration of the cement was accelerated in the fly ash paste compared to the PC paste without fly ash.

5. A number of characteristics of the fly ash pastes undergo discontinuous changes during the period 28 to 90d, manifested by the appearance of maxima or minima in time-dependent parameters observed during this period. Notable in this respect are:

   - the quantity of bound water
   - the quantity of $Ca(OH)_2$ in the paste
   - saturation to $Ca(OH)_2$
   - total pore volume
   - Na, K, SO_4 and OH concentrations in pore water.

   It is clear that major changes in chemical and physical properties occur in the pastes during this time period. These may or may not be related, present data do not permit further conclusions on this issue, although further investigation is clearly required.

6. There are significant indicators that the fly ash is acting chemically as well as physically in the HVFA pastes. First, after reaching a maximum level at ~7d, there is a decline in the calcium hydroxide levels in the HVFA pastes which must be related to

a pozzolanic reaction of the ash. Second, the HVFA pastes have unusually high levels of bound water (~40% at 56d) which must be associated with the formation of hydrates from the fly ash glass. Third, there is a decline in the intensity of the XRD maximum attributed to fly ash glass with advancing curing age.

7. Ettringite (AF_t) is present in greater concentration in the HVFA pastes than the reference PC pastes and is considered to be one product of the short term hydration reactions of the fly ash. A mechanism for the involvement of the alumina and sulphate from the fly ash glass in this reaction has been proposed.

8. Up to 365d, it has not been possible to identify the hydration products formed in the long-term (pozzolanic) reactions of the fly ash glass. That they are not observed in the XRD indicates they have low crystallinity.

9. Etching of the fly ash spheres, while it is observed by SEM in some of the spheres, is not very advanced, even after 365d. It has been proposed that the fly ash in this condition is still reacting, largely by transport of aluminum (and possibly iron) and silanolation/depolymerization of the glassy matrix by the highly alkaline pore fluid. The term "pseudomorphic" has been used to describe the ash spheres at this stage where the overall structural morphology is maintained by the silica network.

10. By virtue of the water reduction through the use of a superplasticizer, the pore fluids in both the HVFA and PC pastes are significantly more concentrated than those of more normal w/c ratio pastes. After 1d, the pore fluid can be considered to be similar to a 1M solution of NaOH and KOH. Both HVFA and PC pastes also show high levels of silicon and sulphate. Unfortunately, the comparison between the two systems is lost after 7d because the pore fluid could not be extracted from the PC pastes.

11. Using a theoretical thermodynamic approach developed by the authors, it has been demonstrated that the pore fluid chemistry in the HVFA pastes is significantly different from the reference PC pastes. The main point of difference between the two systems appears to lie in the control of calcium in solution. Up to 10h, there is extensive supersaturation in the both systems (more pronounced in the PC system) with respect to both $Ca(OH)_2$ and $CaSO_4 \cdot 2H_2O$. Beyond 1d, supersaturation to $Ca(OH)_2$ is still observed in the PC pastes and has been attributed to immobilization of the organo-sulphonate component of the superplasticizer. Similar supersaturation to $Ca(OH)_2$ is not observed in the HVFA pastes between 1 and 90d, although by 365d some supersaturation was observed. More notable is the observation that the HVFA pastes were sub-saturated to $CaSO_4 \cdot 2H_2O$ by some two-orders of magnitude at all ages after 10h. The HVFA pastes seem to have a mechanism for binding OH, Na and K at late ages while maintaining the pore fluids saturated to calcium hydroxide and ettringite.

12. The overall conclusion of this study is that in the HVFA system, physical and chemical factors combine at all ages to densify and bind the paste. In the early stages, the

physical effect of space filling and the chemical contribution to sulphoaluminate production are important; whereas, in the longer term, the pozzolanic hydration reactions dominate as more binder is generated to replace the cement deficiency. This pozzolanic reaction appears to be characterized by high levels of hydration of the fly ash without complete dissolution of the particles. This is interpreted as involving hydrolysis of the fly ash glasses leaving chemically altered pseudomorphic particles in the paste to retain their space filling role.

REFERENCES

1. V.M. Malhotra, "Superplasticized Fly Ash Concrete for Structural Concrete Applications," *Concrete International*, Dec. 1986, pp. 28-31.

2. V.M. Malhotra, "High Volume Fly Ash (Lingan) Concrete for Structural Applications," paper presented at CANMET Seminar: "Nova Scotia Fly Ashes," Halifax, Nova Scotia, Nov. 1986.

3. R. T. Hemmings, E. E. Berry and B. J. Cornelius, "The Use of Beneficiated Lingan Fly Ash for Portland Cement Replacement in Concrete," *ORF Report No. 65-10554*, Nov. 10 1986, for W. S. Langley and Associates.

4. E.E. Berry and R.T. Hemmings, "Beneficiated Lingan Fly Ash: Properties and Applications," paper presented at CANMET Seminar: "Nova Scotia Fly Ashes," Halifax, Nova Scotia, Nov. 1986.

5. E.E. Berry, R.T. Hemmings, W.S. Langley and G. Carette, "Beneficiated Fly Ash: Hydration, Microstructure, and Strength Development in Portland Cement Systems," in *Proc. 3rd Int. Conf. on the Use of Fly Ash, Silica Fume, Slag and Natural Pozzolans in Concrete*, Trondheim, Norway, June 1989, paper SP114-11, pp. 241-273.

6. R.T. Hemmings and B.J. Cornelius, "Characterization of Granulated Blast Furnace Slag for Portland Cement Replacement in Concrete," *ORF Report No. 65-10396* for CANMET (DSS File No. 03SQ.23440-4-9174), Jan. 1986.

7. R.T. Hemmings and E. Douglas, "Characterization of Granulated Blast Furnace Slag for Portland Cement Replacement," *Proc. Int. Workshop on Granulated Blast-Furnace Slag in Concrete*, Oct. 22-23, 1987, pp. 113-153.

8. D. M. F. Orr, "Application of the Scanning Electron Microscope to the Study of the Initial Hydration of Portland Cement Paste," *Cement Conc. Res.*, **13**, 146 (1983).

9. R. T. Hemmings, "Non-Ferrous Slag-Portland Cement Binders: Pozzolanic Activity and Thermal Analysis," *ORF Report No. 65-10251*, Jan. 15 1985, for CANMET (DSS File I5SQ.23440-3-9193).

10. P. Louguet et al., "La Phase Liquid du Ciment Hydrate," *Rev. Materiaux*, **1**, 35 (1973).

11. R. S. Barneyback and S. Diamond, "Expression and Analysis of Pore Fluids from Hardened Cement Pastes and Mortars," *Cement Conc. Res.*, **11**, 279 (1981).

12. E.E. Berry and V.M. Malhotra, "Fly Ash for Use in Concrete Part II — A Critical Review of the Effects of Fly Ash on the Properties of Concrete," *CANMET Report 78-16*, Energy, Mines and Resources Canada, 1978.

13. Proceedings, Symposium on "Effects of Fly Ash Incorporation in Hydrated Cement and Concrete," Editor, S. Diamond, Materials Research Society, Boston, Nov. 16-18, 1981.

14. E.E. Berry and V.M. Malhotra, "Fly Ash for Use in Concrete – A Critical Review," *ACI Journal*, March-April 1980, pp. 59-73.

15. E.E. Berry and V.M. Malhotra, "Fly Ash in Concrete," Energy Mines and Resources Canada Publcn. SP85-3, Feb. 1986.

16. R. Helmuth, "Fly Ash in Cement and Concrete," Portland Cement Association, Skokie, Ill., 1987.

17. S. Diamond, "Cement Paste Microstructure — An Overview at Several Levels," *Proc. Conf. "Hydraulic Cement Pastes: Their Structure and Properties,"* Sheffield, April 8-9, 1976, Cement and Concrete Assocn., Wexham Springs, U.K., pp. 2-23.

18. D.M. Roy and K.M. Parker, "Microstructures and Properties of Granulated Slag–Portland Cement Blends at Normal and Elevated Temperatures," *Proc. CANMET/ACI 1st Conf. on the Use of Fly Ash, Silica Fume, Slag and Other Mineral By-Products in Concrete*, Montebello, Quebec, July 31-Aug 5, 1983, ACI Special Publicn. SP-79, ed. V.M. Malhotra, Vol. I, pp397-413.

19. Papers presented in Symposium P: "Pore Structure and Permeability of Cementitious Materials," Materials Research Society Fall Meeting, Boston, Nov. 28-30. 1988, proceedings in press.

20. F.M. Lea, "The Chemistry of Cement and Concrete, 3rd Ed." Chemical Publishing Company, Inc., N.Y., 1971.

21. S. Diamond, "Effects of Two Danish Fly Ashes on Alkali Contents of Pore Solutions of Cement-Fly Ash Pastes," *Cement Conc. Res.*, **11**, 383 (1981).

22. E.E. Berry and R.T. Hemmings, to be submitted for publication.

23. J.E. Bailey and C.J. Hampson, "The Chemistry of the Aqueous Phase of Portland Cement," *Cement Conc. Res.*, **12**, 227 (1982).

24. E.E. Berry, R.T. Hemmings, B.J. Cornelius and B.E. Scheetz, "Speciation in Size and Density Fractionated Fly Ashes – II. Characterization of a Low-Ca, High-Fe Fly Ash," *Mat. Res. Soc. Proc.*, **86**: "Fly Ash and Coal Conversion By-Products – III" (Materials Research Society, Pittsburgh, 1986), pp. 81-98.

25. E.E. Berry, "Strength Development of Some Blended Cement Mortars," *Cem. Conc. Res.*, **10**, 1 (1980).

26. R.T. Hemmings, E.E. Berry and B.J. Cornelius, "Evaluation of Pozzolanic Applications for Leached Fly Ash," Electric Power Research Institute Report, *EPRI CS-5982/RP2422-17*, August 1988.

27. E.E. Berry, R.T. Hemmings and B.J. Cornelius, "Speciation in Size and Density Fractionated Fly Ashes – III. The Influence of Acid Leaching on a High-Ca Fly Ash," *Mat. Res. Soc. Proc.*, **113**: "Fly Ash and Coal Conversion By-Products – IV" (Materials Research Society, Pittsburgh, 1987), pp. 55-63.

28. R.T. Hemmings and E.E. Berry, "On the Glass in Coal Fly Ashes: Recent Advances," *Mat. Res. Soc. Proc.*, **113**: "Fly Ash and Coal Conversion By-Products – IV" (Materials Research Society, Pittsburgh, 1987), pp. 3-38.

29. R.T. Hemmings and E.E. Berry, "On the Glass in Fly Ashes and Slags: An Overview," paper presented at the *2nd Int. Conf. on the Use of Fly Ash, Silica Fume, Slag and Natural Pozzolans in Concrete*, Madrid, Spain, April 1986.

30. A. Verhasselt, "Characterization of the Pozzolanicity of Fly Ash," in *Proc.7th Int. Cong. on the Chemistry of Cement*, Vol III, pp.IV-116-121, Paris, Paris Editions Septima, 1980.

31. R. Sersale and P.G. Orsini, "Hydrated Phases after Reaction of Lime with Pozzolanic Materials or with Blast Furnace Slags," *Proc. 5th Int. Symp. on the Chemistry of Cement*, Tokyo, 1968, Part IV, pp. 114-121.

32. R. Dron, "Experimental and Theoretical Study of the $CaO–Al_2O_3–SiO_2–H_2O$ System," *6th Int. Conf. on the Chemistry of Cement*, Moscow, 1974, supplementary paper 9-5.

33. R. Dron, "Les Pouzzolanes et la Pouzzolanicité," *Rev. des Materiaux de Construction*," No. 692, pp. 27-30 (1975).

34. E.E. Lachowski, K. Mohan and H.F.W. Taylor, "Analytical Electron Microscopy of Cement Pastes, II. Pastes of Portland Cement and Clinkers," *J. Am. Ceram. Soc.*, **63**, 447 (1980).

35. R. Sersale, "Structure and Characterization of Pozzolanas of Fly Ash," *Proc.7th Int. Cong. on the Chemistry of Cement*, Vol I, pp.IV-1/3-18, Paris Editions Septima, 1980.

36. F. Masazza, "Chemistry of Pozzolanic Additions and Mixed Cements," *6th Int. Conf. on the Chemistry of Cement*, Moscow, 1974, principal paper III-6; ibid. Il cemento, 73, pp. 3-39 (1976).

37. S. Diamond, "Methodology of PSD Measurement in HCP: Postulates, Peculiarities, and Problems," presented at Fall Meeting of the Materials Research Society, Symposium P, paper P2.4, Boston, Nov. 28-30, 1988.

TABLES

Table 1

PROPERTIES OF PORTLAND CEMENT AND FLY ASH

Property	Portland Cement*	Fly Ash†
Chemical Analysis (mass %):		
SiO_2	21.2	43.2
Al_2O_3	4.1	21.0
Fe_2O_3	2.8	24.2
CaO	62.2	1.6
MgO	3.8	1.0
Na_2O	0.5	0.5
K_2O	1.0	2.2
MnO	–	0.1
TiO_2	–	0.9
P_2O_5	–	0.2
Carbon	0.3	1.9
SO_3	3.0	1.3
Loss on ignition	1.6	3.3
Calculated Composition (Bogue):		
C_3S	51.6	–
C_2S	22.0	–
C_3A	6.1	–
C_4AF	8.5	–
$CaCO_3$**	2.3	–
Physical Properties:		
Fineness, % -45 µm	92.8	86.4
Mean particle size, µm	–	10.1
28d Pozzolanic index with PC, %	–	83.8
Water requirement, %	–	97.7
Autoclave expansion, %	0.16	+0.001
Compressive strength, MPa		
3d	25.1	17.1§
7d	31.5	20.1§
28d	39.3	29.3§

* Data provided by CANMET.

† From reference 3.

** Calculated from TGA/DTG data (this study)

§ 30% replacement of PC with fly ash

Table 2

CHEMICAL ANALYSIS OF SUPERPLASTICIZER

Component	% by mass
SiO_2	0.1
Al_2O_3	0.1
Fe_2O_3	<0.02
CaO	0.3
MgO	<0.02
Na_2O	13.8
K_2O	<0.1
TiO_2	<0.1
MnO	<0.01
Carbon	49.6
Sulphur	11.1
Sulphonate	27.8
Sulphate	15,500 mg/L
Solids content	41.2

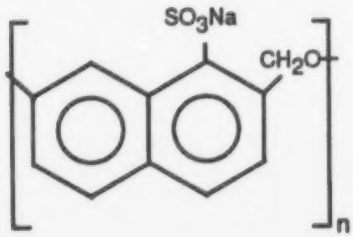

Sodium salt of sulphonated naphthalene formaldehyde

Table 3

MIX PROPORTIONS FOR PASTE AND MORTAR SPECIMENS

	Mortar			Paste	
	C109	PC_{sp}	PC–FA_{sp}	PC_{sp}	PC–FA_{sp}
Cement (g)	250	1925	808.5	1700	714
Sand (g)	687.5	5294	5294	–	–
Fly Ash (g)	–	–	1116.5	–	986
Water (mL)	116	548.6	565.4	484.5	499.4
Superplasticizer (mL)	–	49.1	20.6	43.3	18.2
w/c	0.464	0.300	0.715	0.300	0.715
w/c+f	0.464	0.300	0.300	0.300	0.300
Flow	108.5	no flow	37	–	–

Table 4

COMPRESSIVE STRENGTH DEVELOPMENT IN TEST MORTARS

Sample Age	ASTM C109 Mortar		·····Superplasticized Mortars····· PC Mortar		PC–FA Mortar	
	MPa	*psi*	*MPa*	*psi*	*MPa*	*psi*
1d	15.3	(2217)	33.2	(4811)	10.3	(1492)
3d	24.6	(3560)	41.1	(5955)	20.5	(2973)
7d	29.3	(4247)	45.9	(6659)	26.2	(3805)
14d	32.8	(4763)	49.0	(7109)	32.8	(4750)
28d	38.2	(5546)	53.7	(7783)	38.2	(5538)
90d	41.1	(5967)	62.9	(9125)	50.9	(7375)
365d	44.1	(6400)	63.6	(9225)	62.9	(9125)
Mortar Flow	108.5		no flow		37	

Table 5

MERCURY INTRUSION POROSIMETRY DATA FOR PASTES

Sample	Total Pore Area (m^2/g)	Average Pore Diameter (μm)	Bulk Density (g/cm^3)	Skeletal Density (g/cm^3)	Porosity (%)
PC Pastes:					
2h	12.1	0.10	1.6	3.1	47.7
5h	9.4	0.13	1.6	3.1	48.2
10h	23.0	0.04	1.8	3.2	44.9
1d	46.5	0.02	1.9	2.7	32.4
3d	45.7	0.01	1.9	2.6	27.6
7d	47.6	0.01	1.9	2.6	25.9
14d	45.4	0.01	2.0	2.7	26.5
28d	44.1	0.01	2.0	2.6	24.1
56d	38.9	0.04	2.0	2.6	21.9
90d	51.1	0.01	2.0	2.7	24.9
365d	34.4	0.01	1.9	2.4	21.1
PC–FA Pastes:					
2h	11.8	0.10	1.5	2.9	48.3
5h	11.9	0.10	1.5	2.9	46.9
10h	11.3	0.11	1.5	2.9	47.0
1d	29.7	0.03	1.6	2.7	39.9
3d	39.4	0.02	1.6	2.6	36.5
7d	45.6	0.02	1.7	2.6	32.5
14d	52.0	0.02	1.7	2.7	35.3
28d	32.2	0.02	1.7	2.1	21.7
56d	50.5	0.01	1.8	2.5	27.7
90d	62.2	0.01	1.9	2.7	30.6
365d	86.6	0.01	1.8	2.8	36.8

Table 6

X-RAY POWDER DIFFRACTION DATA FOR PASTES

Sample	·····Relative Intensity for Selected Peak for Given Phase*·····				
	C_3S	C_2S	Quartz	CH	$C_3A{\cdot}3CS{\cdot}32H_2O$
PC Pastes:					
2h	78	7	–	–	7
5h	74	10	–	–	6
1d	61	8	–	100	25
3d	58	8	–	100	14
7d	78	–	–	100	19
14d	52	–	–	100	12
28d	48	18	–	100	23
90d	48	6	–	100	–
365d	44	22	–	71	15
PC–FA Pastes:					
2h	96	8		–	–
5h	52	–	100	–	16?
1d	32	–	100	55	30?
3d	20	–	100	98	33
7d	18	–	100	85	28?
14d	–	–	64	95	22?
28d	29	14?	100	72	23?
90d	15	11	100	36	–
365d	35	28?	100	42	17?

* Diffraction lines used for intensity measurements:
C_3S, 3.02Å; quartz, 3.34Å; C_2S, 2.88Å; CH (calcium hydroxide), 2.63Å;
$C_3A{\cdot}3CS{\cdot}32H_2O$ (ettringite), 9.73Å.

Table 7

CALCIUM HYDROXIDE AND BOUND WATER CONTENTS OF PASTES*

Sample Age	Grams per 100g Total Binder $Ca(OH)_2$	Grams per 100g Total Binder Bound H_2O	Grams per 100g OPC $Ca(OH)_2$	Grams per 100g OPC Bound H_2O
PC Pastes:				
2h	0.4	1.8	0.4	1.8
5h	0.6	2.5	0.6	2.5
10h	3.6	6.6	3.6	6.6
1d	11.6	14.7	11.6	14.7
3d	10.6	14.6	10.6	14.6
7d	15.1	15.5	15.1	15.5
14d	14.6	16.4	14.6	16.4
28d	15.7	17.5	15.7	17.5
56d	16.6	19.1	16.6	19.1
90d	12.9	18.3	12.9	18.3
365d	17.2	19.8	17.2	19.8
PC–FA Pastes:				
2h	0.2	2.2	0.5	6.8
5h	0.3	2.2	0.9	6.8
10h	0.5	3.5	1.5	10.7
1d	3.6	6.9	11.3	21.5
3d	5.7	10.2	17.5	31.6
7d	6.6	9.1	20.5	28.1
14d	6.5	11.8	20.1	36.6
28d	5.6	11.3	17.3	34.9
56d	6.9	17.8	21.2	54.9
90d	4.7	13.7	14.3	42.4
365d	3.6	9.8	11.3	30.2

* Calculated from TGA/DTG data.

Table 8

ANALYTICAL CONCENTRATIONS OF EXTRACTED PORE SOLUTIONS

Sample (Age)	pH*	Ionic Concentration (mmol/l) Si	Ca	Al	Na	K	SO_4	OH	Cations / Anions †
PC Pastes:§									
2h	13.32	1.9	34.9	1.7	396	336	242	209	1.18
5h	13.30	0.4	3.0	0.1	407	358	254	200	1.09
10h	13.42	1.2	0.5	0.1	440	429	297	266	1.02
1d	13.99	36.6	5.2	0.6	653	621	73.7	981	1.26
3d	14.06	12.1	5.4	1.1	678	616	45.6	1149	1.09
7d	14.07	10.9	8.4	1.3	744	672	66.8	1174	1.13
PC–FA Pastes:									
2h	13.05	0.6	16.1	0.2	196	93	152	112	0.78
5h	13.16	0.4	17.2	<0.1	207	91	138	144	0.79
10h	13.29	0.5	0.6	<0.1	219	212	125	194	0.98
1d	13.71	0.7	0.5	0.2	301	257	8.7	511	1.07
3d	13.80	1.3	0.8	0.2	383	313	6.8	634	1.09
7d	13.81	0.6	2.9	0.4	381	158	12.2	653	0.81
14d	13.69	3.1	1.5	0.9	296	256	17.8	494	1.08
28d	13.66	13.8	2.5	3.5	277	333	12.9	454	1.41
56d	13.66	7.7	2.5	3.8	268	264	16.5	457	1.18
90d	13.58	6.1	2.7	3.7	229	256	19.3	384	1.24
365d	15.57	26.7	12.5	4.6	299	192	29.1	375	1.47

* pH calculated from titration of solution to methylred endpoint.

† $\frac{\text{Cations}}{\text{Anions}} = \frac{(4Si + 2Ca + 3Al + Na + K)}{(2SO_4 + OH)}$

§ Data not available beyond 7d since pore fluids could not be extracted.

Table 9

TOTAL SODIUM, POTASSIUM AND SULPHATE CONTAINED IN PASTE MATERIALS

(mmol/L OF MIX WATER)

Paste Mix	mmol/L		
	Na	K	SO_4
PC_{sp}	606	549	1,345
$PC–FA_{sp}$	560	1,119	849

Table 10

Na, K, SO_4 AND OH QUANTITIES (mmol/100g of paste)

IN EXTRACTED PORE SOLUTIONS

Sample	PC Pastes*				PC–FA Pastes			
Age	Na	K	SO_4	OH	Na	K	SO_4	OH
2h	8.6	7.3	5.3	4.5	4.1	1.9	3.2	2.3
5h	8.6	7.6	5.4	4.2	4.3	1.9	2.9	3.0
10h	7.9	7.7	5.4	4.8	4.3	4.2	2.5	3.8
1d	7.7	7.3	0.86	11.5	4.9	4.2	0.14	8.2
3d	8.0	7.3	0.54	13.6	4.9	4.0	0.09	8.2
7d	8.3	7.5	0.74	13.1	5.3	2.2	0.17	9.1
14d	–	–	–	–	3.3	2.9	0.20	5.6
28d	–	–	–	–	2.7	3.9	0.15	5.4
56d	–	–	–	–	1.4	1.4	0.09	2.4
90d	–	–	–	–	2.1	2.4	0.18	3.6
365d	–	–	–	–	4.0	2.6	0.39	5.0

* Data not available beyond 7d since pore fluids could not be extracted.

Table 11

CALCULATED IONIC CONDITIONS IN PORE FLUIDS FROM SUPERPLASTICIZED PC PASTES

Parameter	Curing Age 2hr	5hr	10hr	1d	3d	7d
Ionic Strength (mmol/L):						
Total	372	398	471	560	617	647
Ca^{2+}	6	5	1	5	4	6
Na^{+}	347	352	375	634	666	726
K^{+}	264	276	324	588	596	642
SO_4^{2-}	104	115	127	217	13	18
OH^{-}	197	199	266	977	1144	1167
$(CaOH)^{+}$	11.6	0.9	0.2	4.5	4.8	7.5
$(CaSO_4)^{0}$	17.1	1.5	0.3	0.3	0.2	0.3
$(NaSO_4)^{-}$	49.5	55.4	64.8	18.8	12.1	18.3
$(KSO_4)^{-}$	71.9	82.4	105.4	32.9	20.3	30.3
Cat/Anion	1.21	1.11	1.01	0.84	1.05	1.10
Activity Products (x 10^{-6}):†						
$Ca(OH)_2$	48	3.97	1.08	91	116	183
$CaSO_4.2H_2O$	72.6	6.48	1.09	1.18	0.66	1.39
Calculated Saturation Factors:						
$Ca(OH)_2$	7.43	0.61	0.17	14.09	17.96	28.33
$CaSO_4.2H_2O$	27.92	2.49	0.42	0.45	0.26	0.53

† Published values of equilibrium saturation products are [23]:

$Ca(OH)_2$	6.46×10^{-6}
$CaSO_4.2H_2O$	2.60×10^{-6}

Table 12

CALCULATED IONIC CONDITIONS IN PORE FLUIDS FROM SUPERPLASTICIZED PC–FA PASTES

Parameter	Curing Age 2hr	5hr	10hr	1d	3d	7d	14d	28d	56d	90d	365d
Ionic Strength (mmol/L):											
Total	275	268	264	266	325	342	268	242	248	215	223
Ionic Concentration (mmol/L):											
Ca^{2+}	3.4	3.6	0.1	0.1	0.1	0.4	0.3	0.5	0.5	0.6	2.5
Na^{+}	172	184	199	299	382	378	292	275	265	226	293
K^{+}	73	73	177	254	311	155	250	328	258	249	184
SO_4	98	88	70	4.1	2.8	6.2	8.4	5.4	7.7	9.2	14.1
OH^{-}	108	139	194	511	633	651	493	452	455	382	366
$(CaOH)^{+}$	3.5	4.8	0.2	0.4	0.7	2.5	1.2	2.0	2.0	2.0	8.9
$(CaSO_4)^{0}$	9.2	8.8	0.2	0.0	0.0	0.1	0.1	0.1	1.0	2.0	1.0
$(NaSO_4)^{-}$	24.5	23.4	20.4	1.7	1.6	3.3	3.6	2.2	3.1	3.2	6.4
$(KSO_4)^{-}$	20.0	18.0	34.7	2.9	2.4	2.6	5.8	5.2	5.7	6.8	7.6
Cat/Anion	0.73	0.75	0.97	1.06	1.08	0.80	1.05	1.29	1.10	1.17	1.2
Activity Products (x 10^{-6}):†											
$Ca(OH)_2$	8.2	14.0	1.0	4.5	9.5	34.1	12.9	19.5	19.4	17.2	72.0
$CaSO_4.2H_2O$	3910	37.4	1.12	0.04	0.04	0.28	0.25	0.30	0.41	0.63	0.44
Saturation Factors:											
$Ca(OH)_2$	1.27	2.17	0.16	0.70	1.47	5.28	2.00	3.02	3.00	2.66	11.14
$CaSO_4.2H_2O$	15.0	14.4	0.43	0.01	0.01	0.11	0.09	0.11	0.15	0.24	1.69

† Published values are [23]:

$Ca(OH)_2$	6.46×10^{-6}
$CaSO_4.2H_2O$	2.60×10^{-6}

Table 13

SUMMARY OF EARLY AGE CHEMICAL CONDITIONS IN PASTES

Sample	·····PC Pastes*·····				·····PC–FA Pastes·····			
Age	5h	10h	1d	3d	5h	10h	1d	3d
Saturation Factors:								
$Ca(OH)_2$	0.6	0.2	14	18	2.2	0.2	0.7	1.5
Gypsum	2.5	0.4	0.5	0.3	14.1	0.4	0.01	0.01
Quantities in solution (mmol/100g paste):								
Na	8.6	8.6	7.9	7.7	4.3	4.3	4.9	4.9
K	7.3	7.6	7.7	7.3	1.9	4.2	4.2	4.0
SO_4	5.3	5.4	5.4	0.86	2.9.	2.5	0.14	0.1
OH	4.5	4.2	4.8	11.5	3.0	3.8	8.2	8.2
Solid phases:								
% $Ca(OH)_2$	0.6	3.6	11.6	10.6	0.3	0.5	3.6	5.7
Gypsum	None detected							
AF_t	Detected but not quantified							

FIGURES

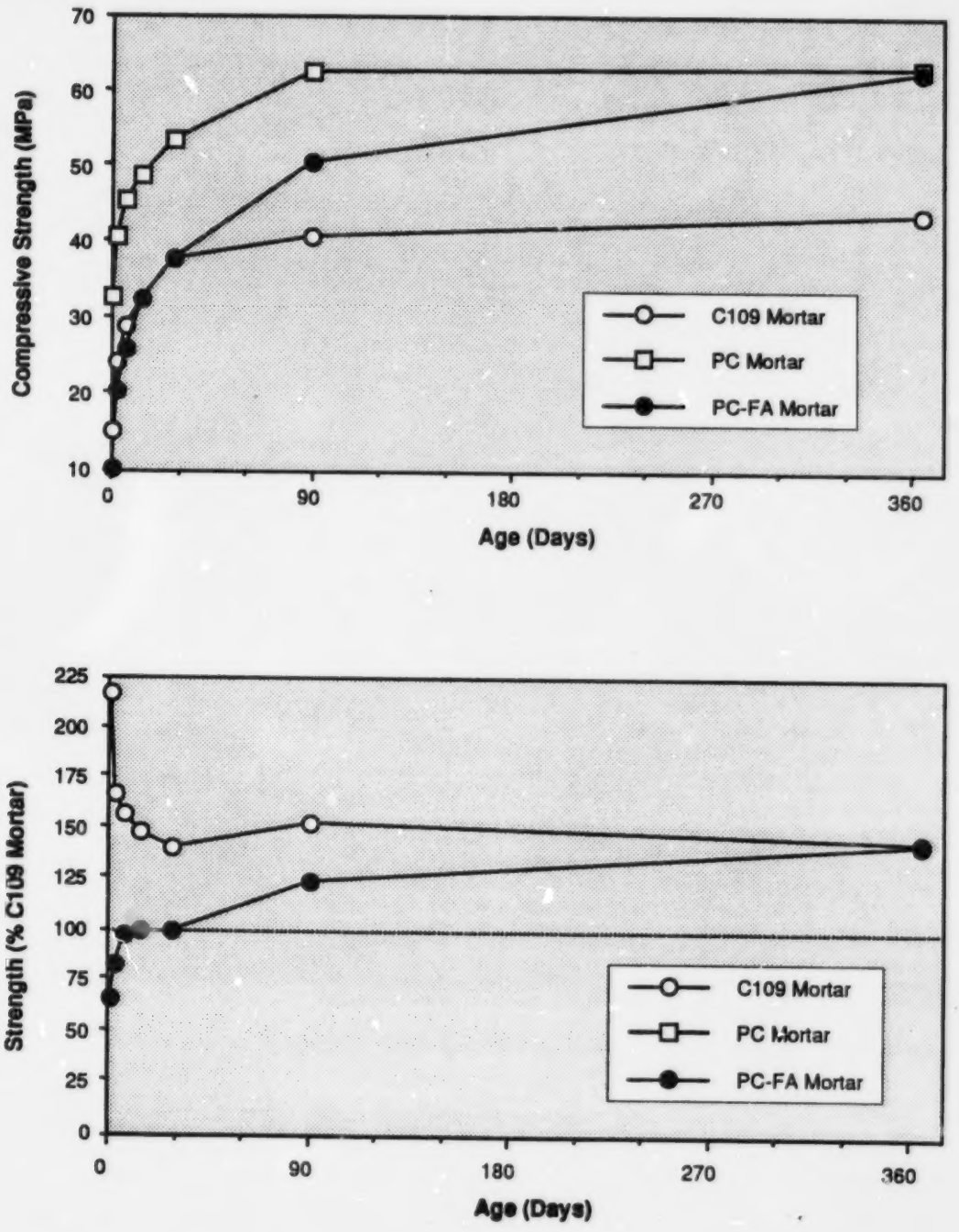

Figure 1. Strength development in superplasticized mortars: upper graph, absolute strength; lower graph, strength relative to ASTM C109 mortar.

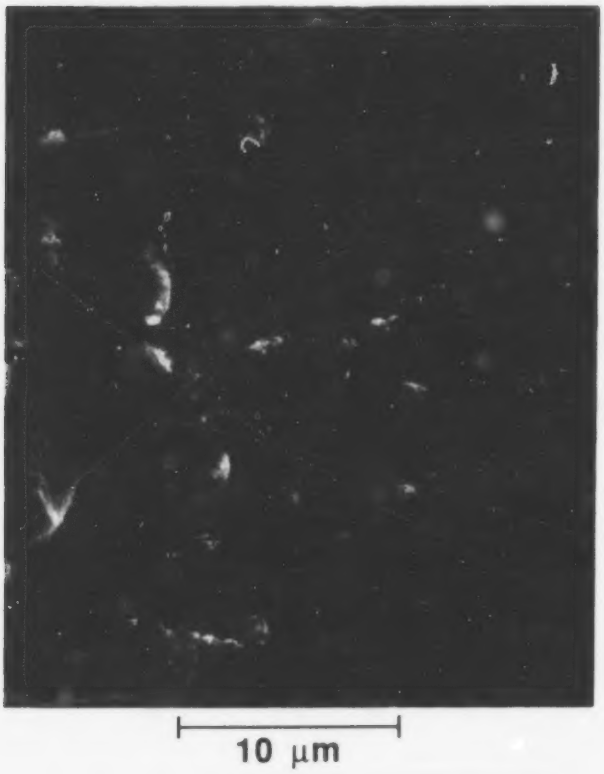

Figure 2a. Scanning electron micrographs of fracture surfaces of PC_{sp} pastes at 10h.

Figure 2b. Scanning electron micrographs of fracture surfaces of PC–FA$_{sp}$ pastes at 10h.

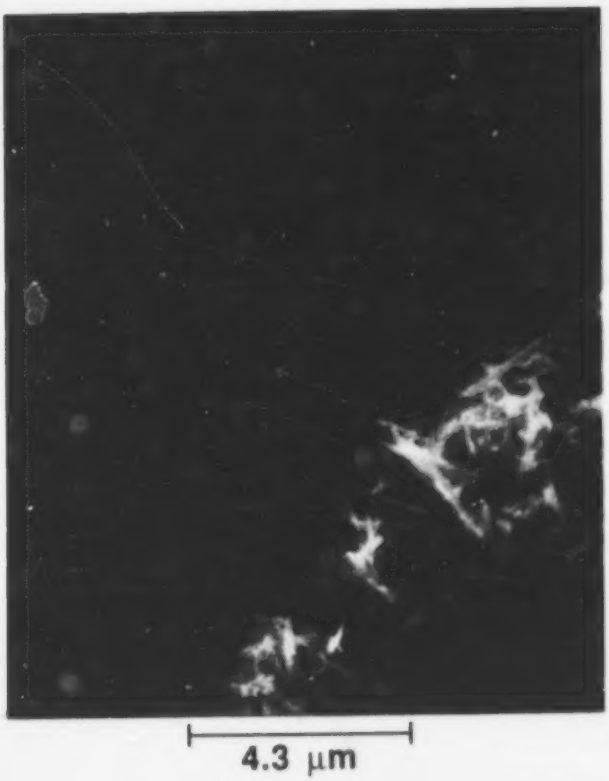

Figure 2c. Scanning electron micrographs of fracture surfaces of PC_{sp} pastes at 3d.

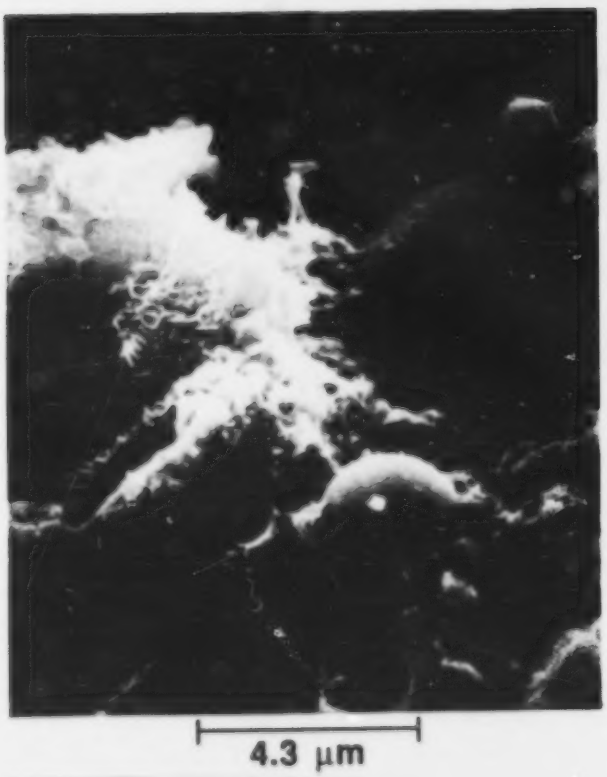

Figure 2d. Scanning electron micrographs of fracture surfaces of PC–FA_{sp} pastes at 3d.

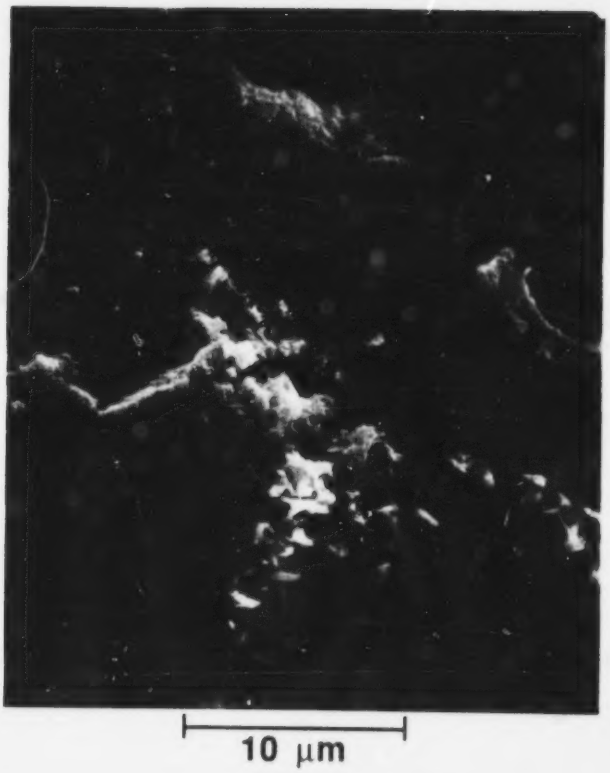

Figure 2e. Scanning electron micrographs of fracture surfaces of PC_{sp} pastes at 28d.

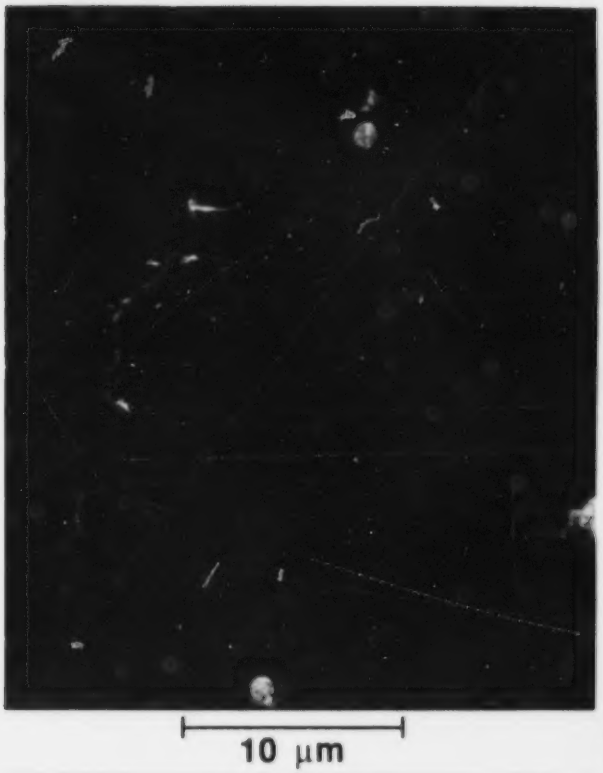

Figure 21. Scanning electron micrographs of fracture surfaces of PC–FA_{sp} pastes at 28d.

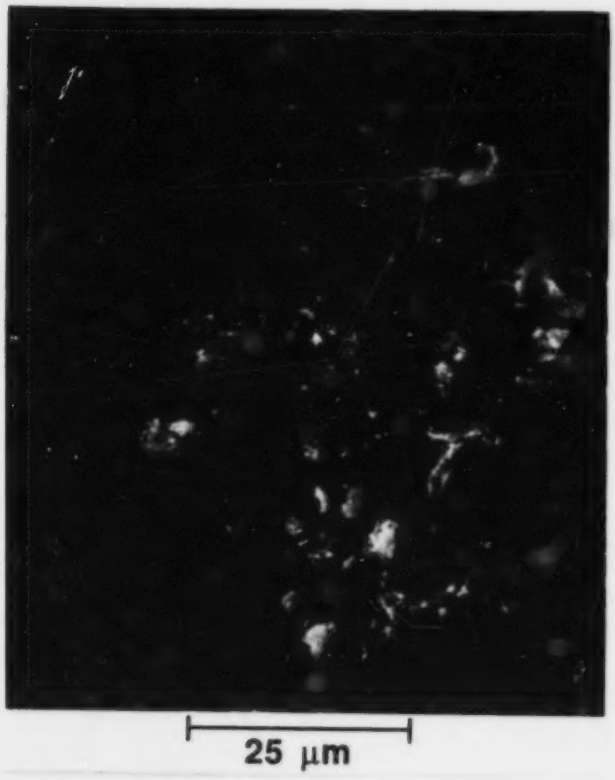

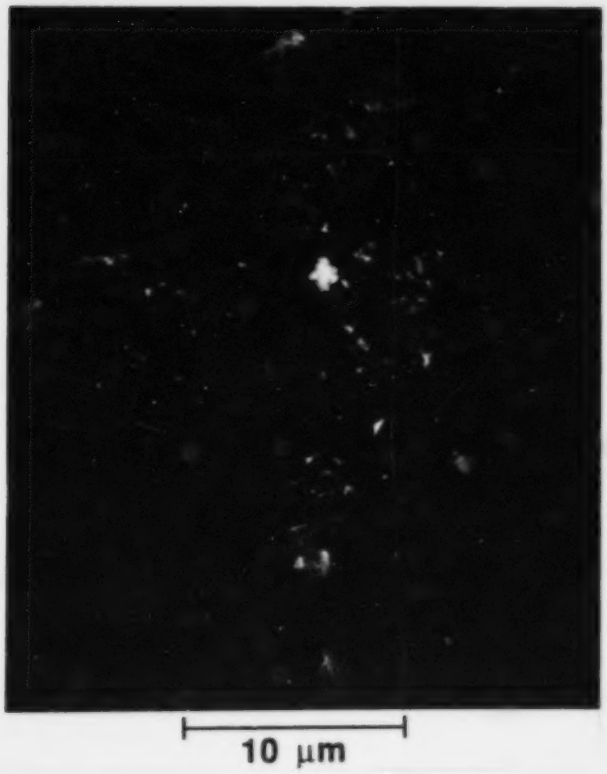

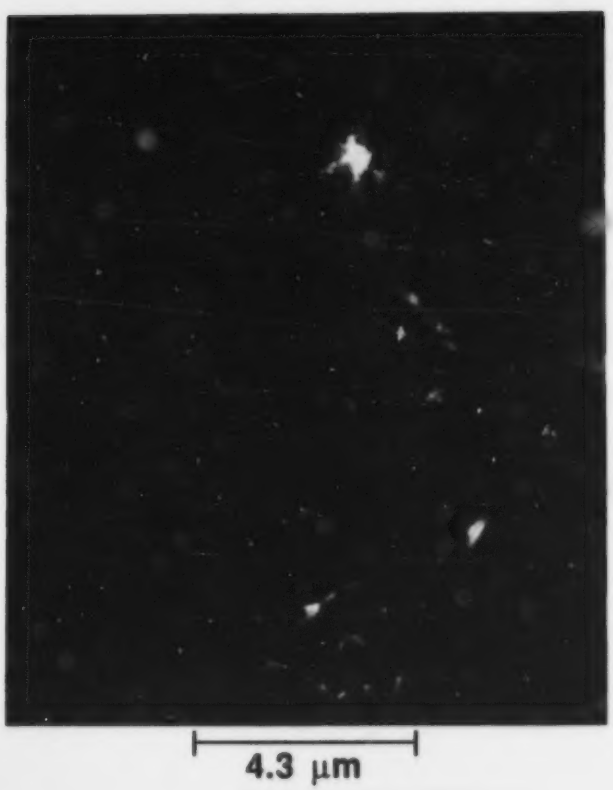

Figure 2g. Scanning electron micrographs of fracture surfaces of PC_{sp} pastes at 90d.

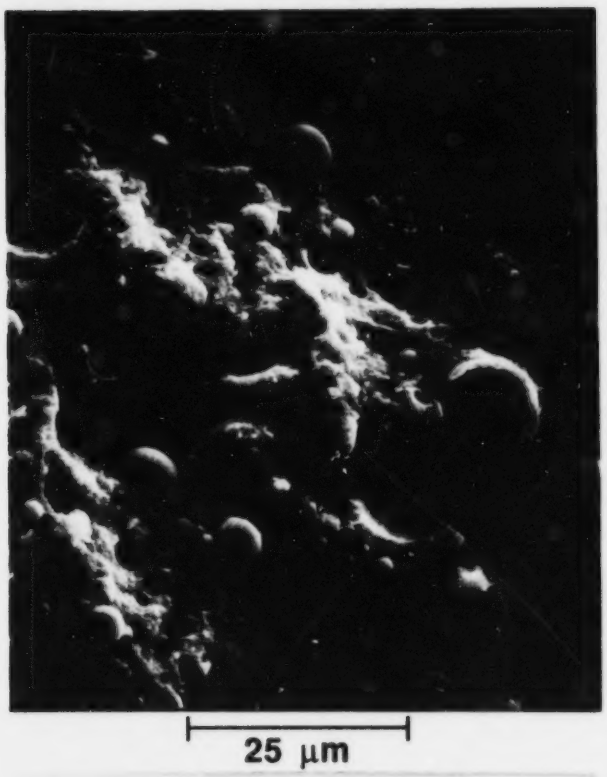

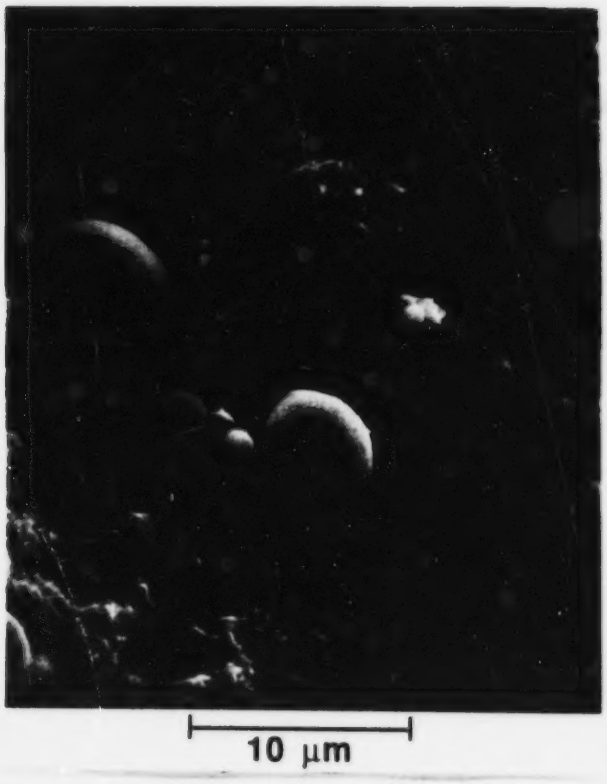

Figure 2h. Scanning electron micrographs of fracture surfaces of PC–FA_{sp} pastes at 90d.

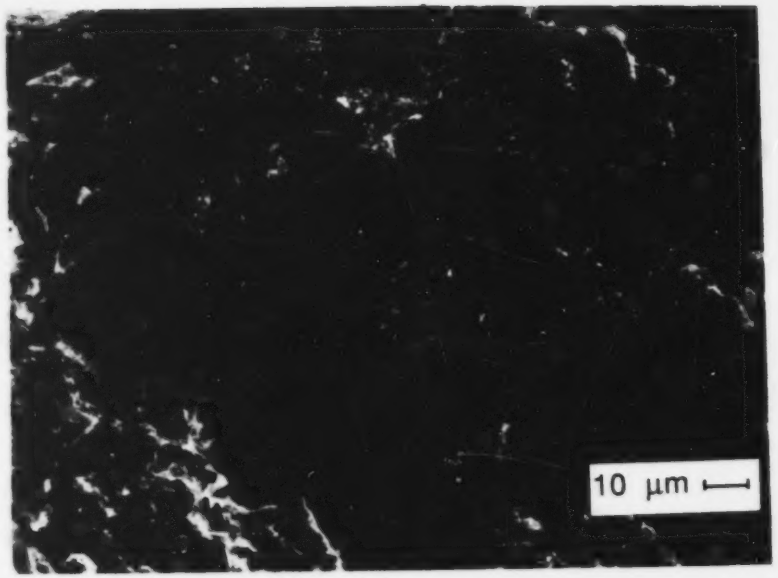

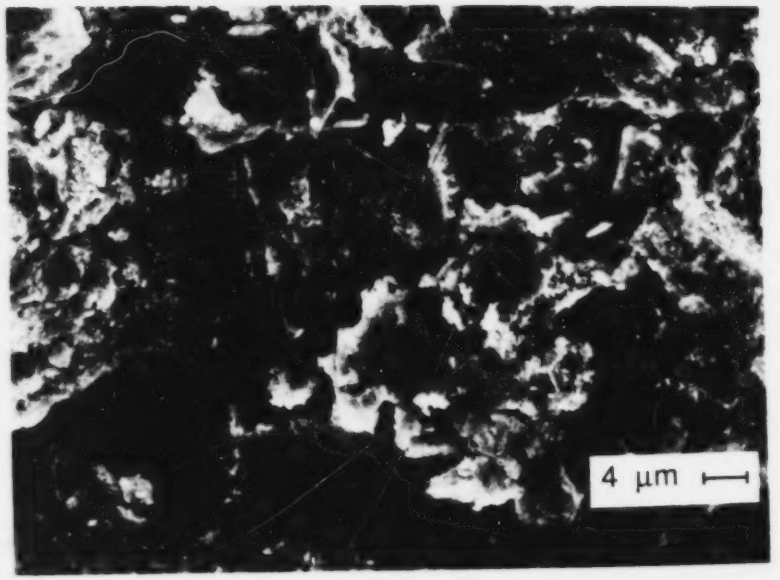

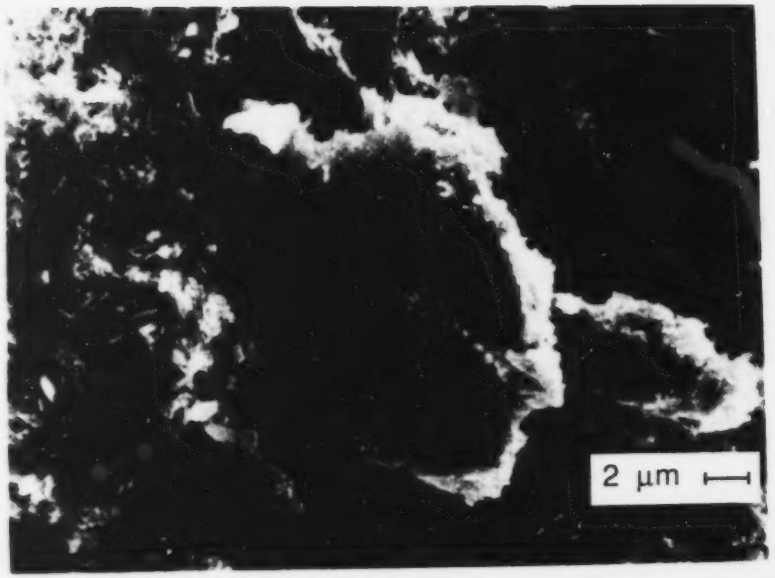

Figure 2i. Scanning electron micrographs of fracture surfaces of PC_{sp} pastes at 365d.

Figure 2j. Scanning electron micrographs of fracture surfaces of PC–FA_{sp} pastes at 365d.

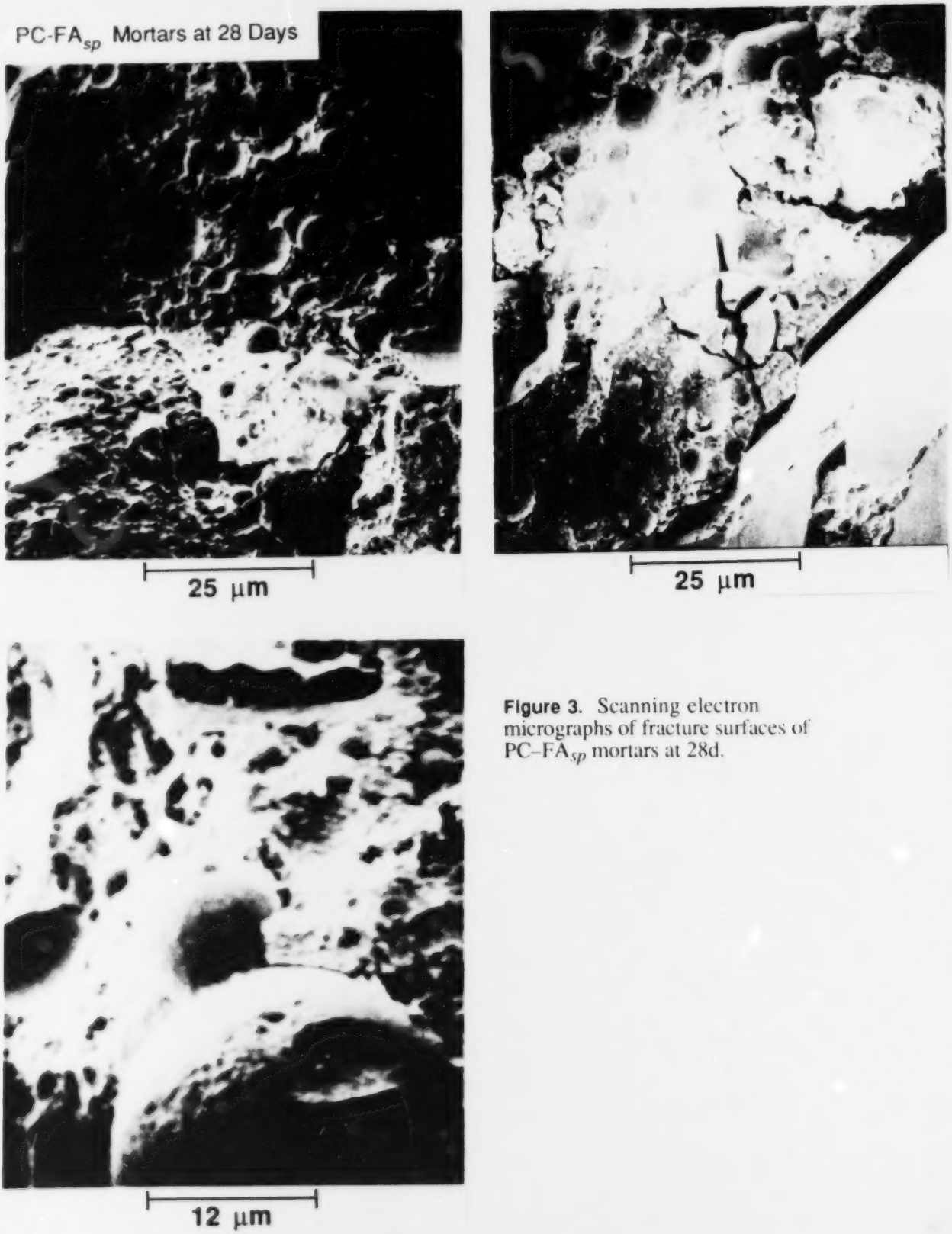

Figure 3. Scanning electron micrographs of fracture surfaces of PC–FA$_{sp}$ mortars at 28d.

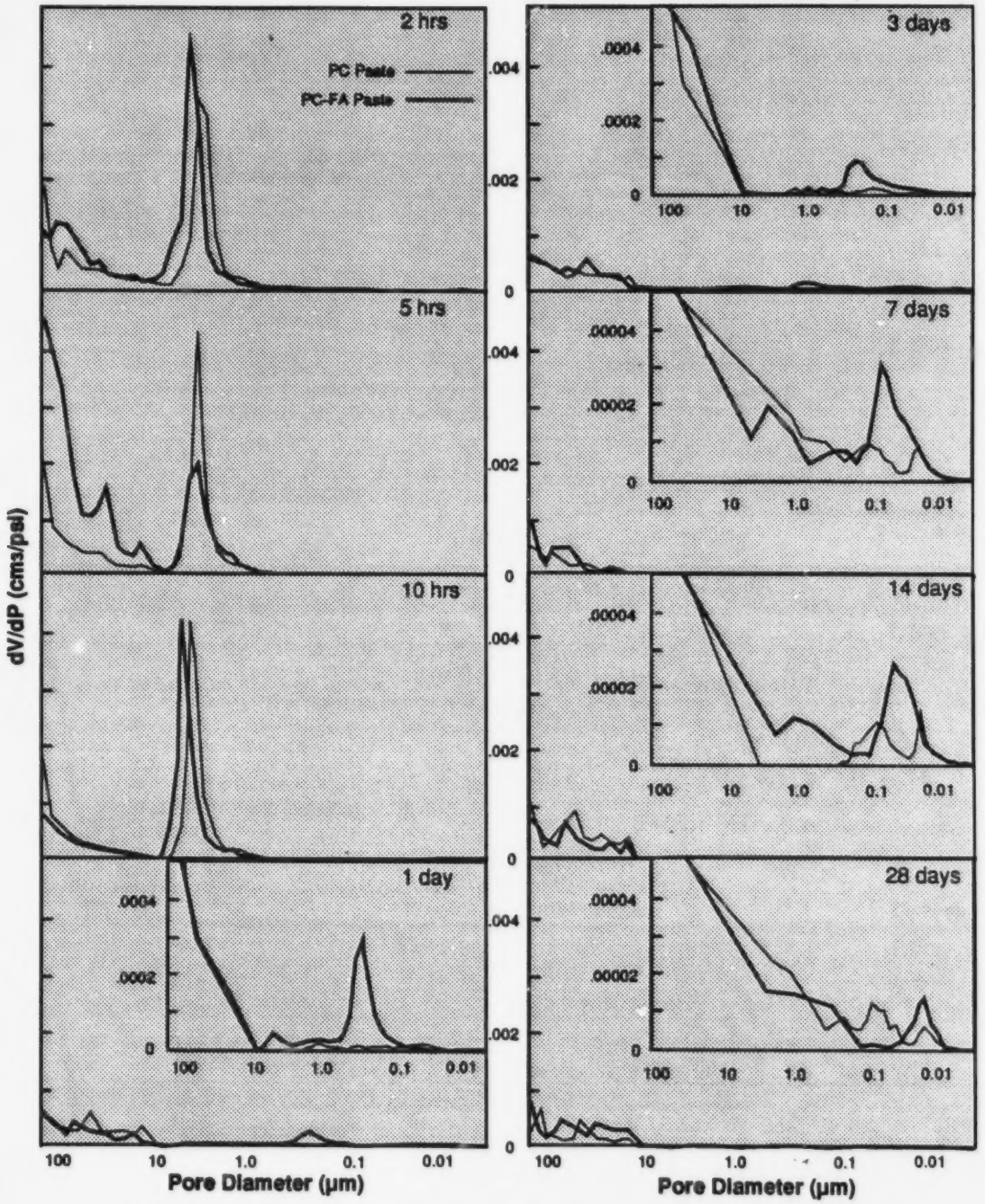

Figure 4a. Variation of dV/dP with pore diameter for PC and PC–FA pastes at curing ages from 2h to 28d. Insets show intrusion profiles with vertical axis expanded to show low level detail.

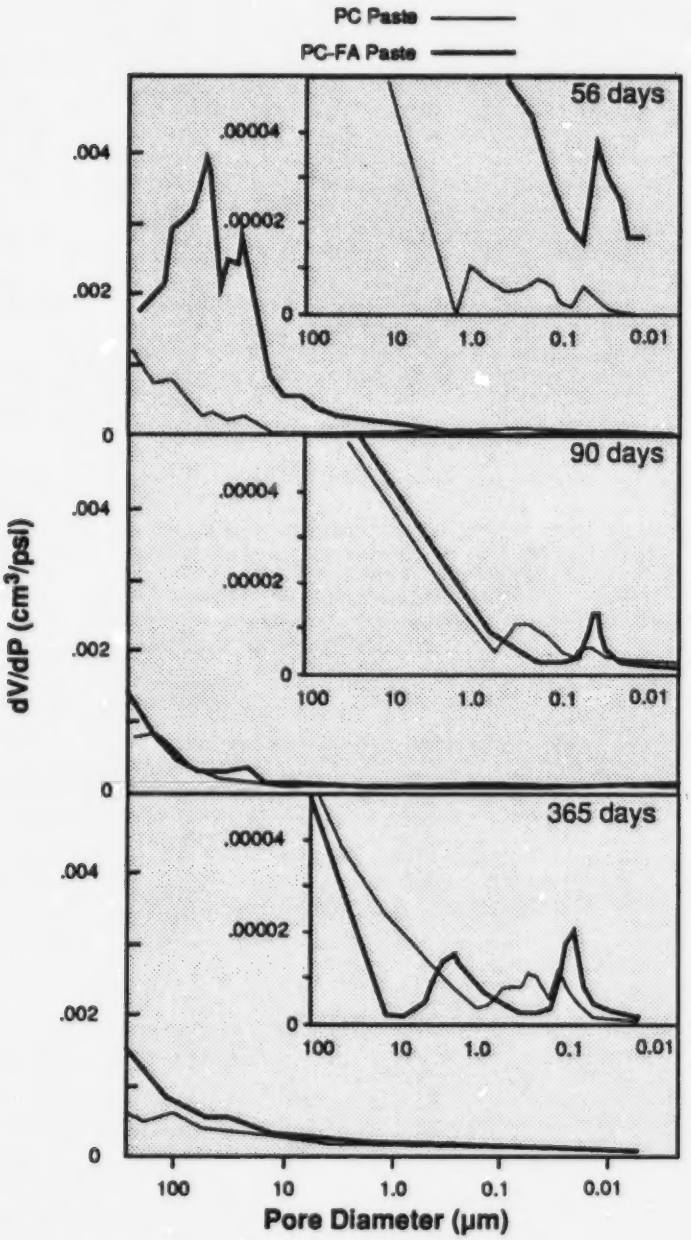

Figure 4b. Variation of dV/dP with pore diameter for PC and PC–FA pastes at curing ages of 56d, 90d and 365d. Insets show intrusion profiles with vertical axis expanded to show low level detail.

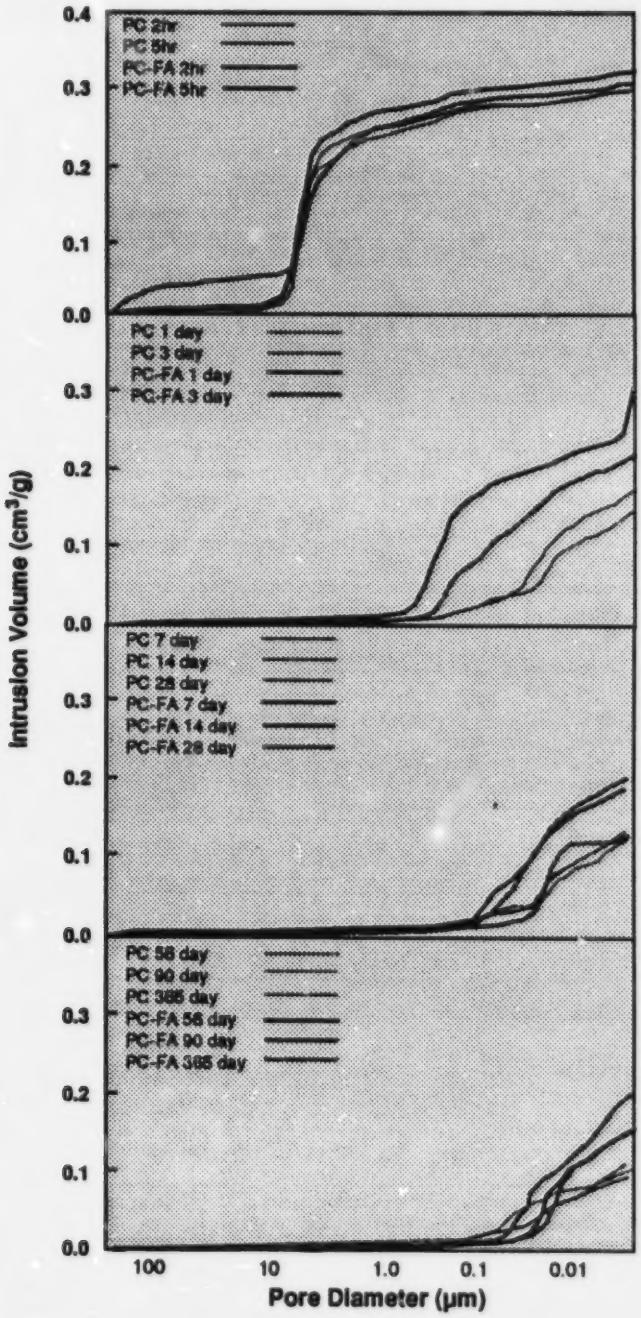

Figure 5. Cumulative pore volume vs. pore diameter for PC and PC–FA pastes plotted as absolute intrusion volume.

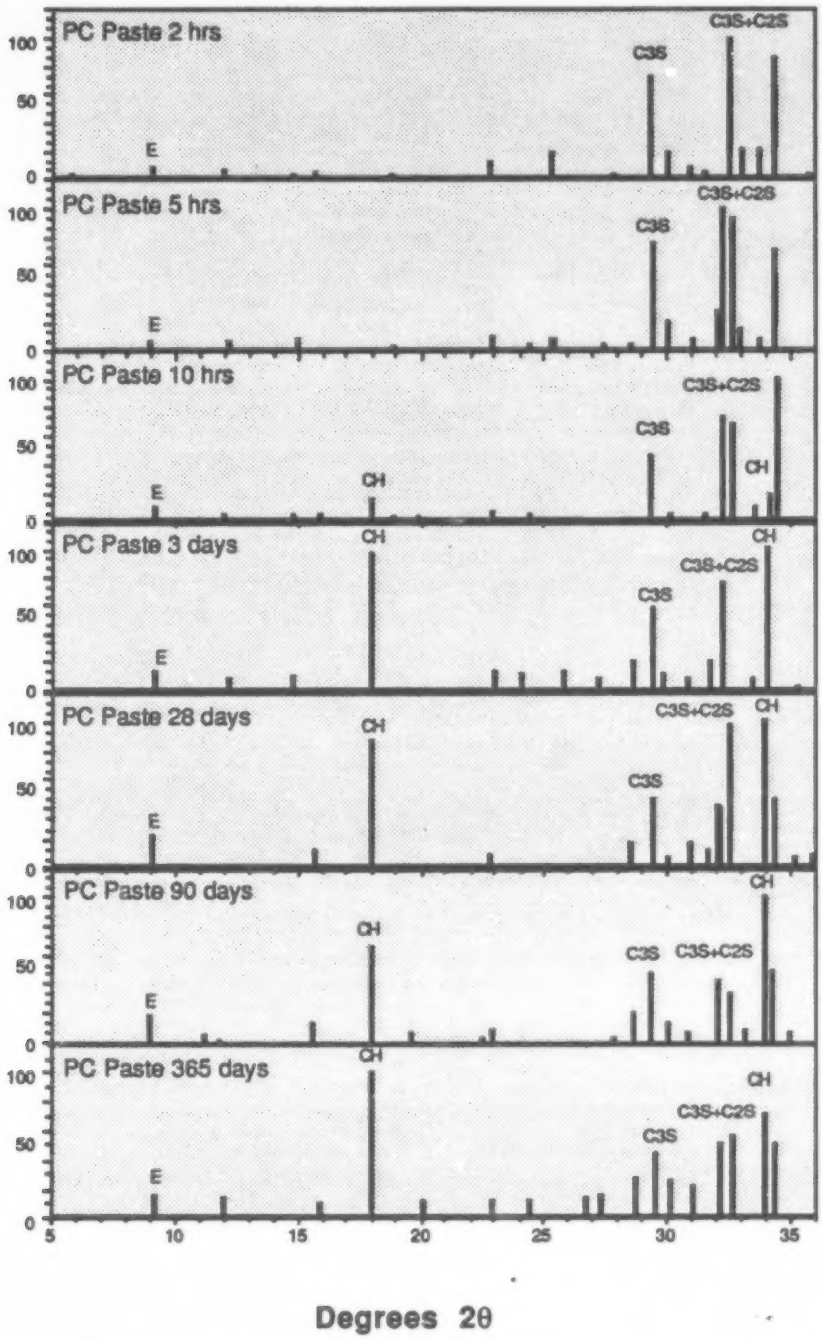

Figure 6. Computer enhanced XRD patterns (CuK_α) for superplasticized PC pastes. Phases identified as follows: **E**, ettringite; **CH**, calcium hydroxide; **C_3S**, tricalcium silicate; **C_2S**, dicalcium silicate.

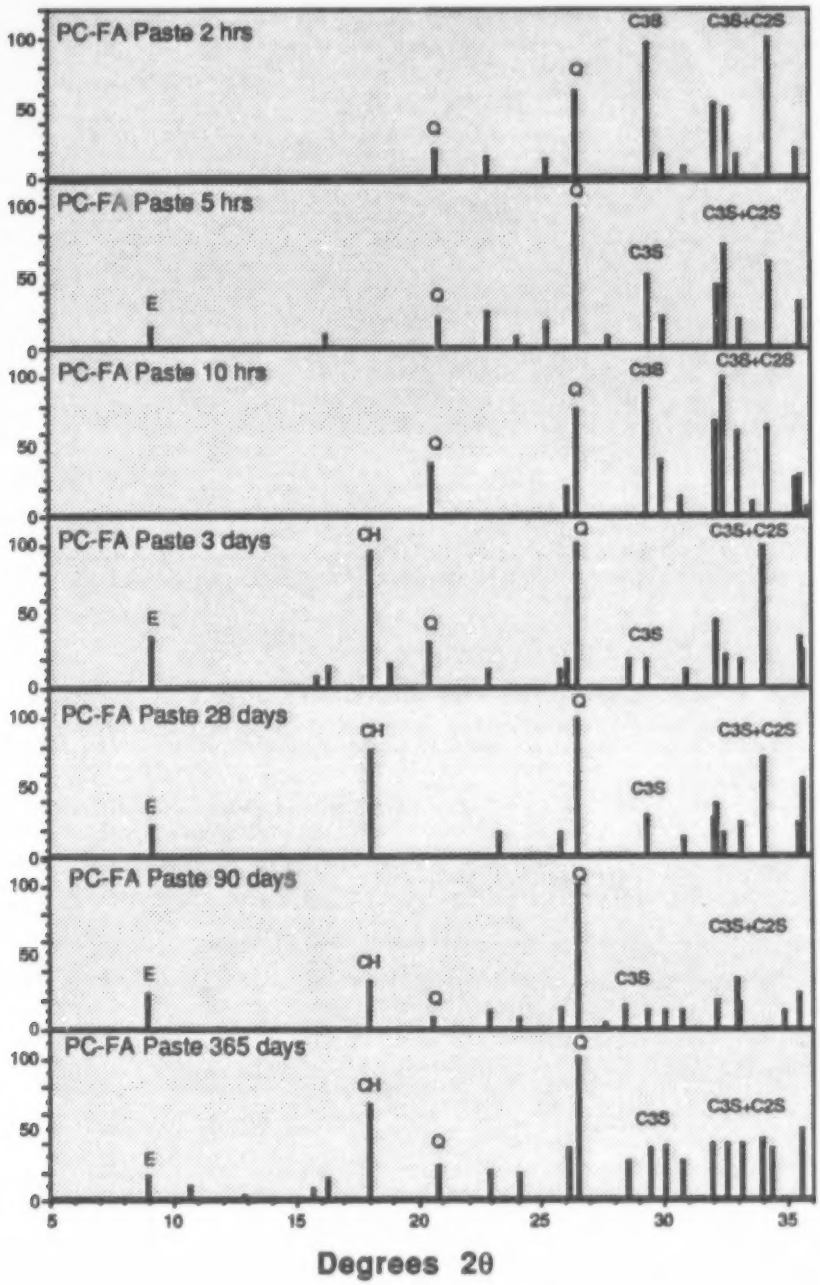

Figure 7. Computer enhanced XRD patterns (CuK_α) for superplasticized PC–FA pastes. Phases identified as follows: **E**, ettringite; **CH**, calcium hydroxide; **C_3S**, tricalcium silicate; **C_2S**, dicalcium silicate; **Q**, quartz (fly ash).

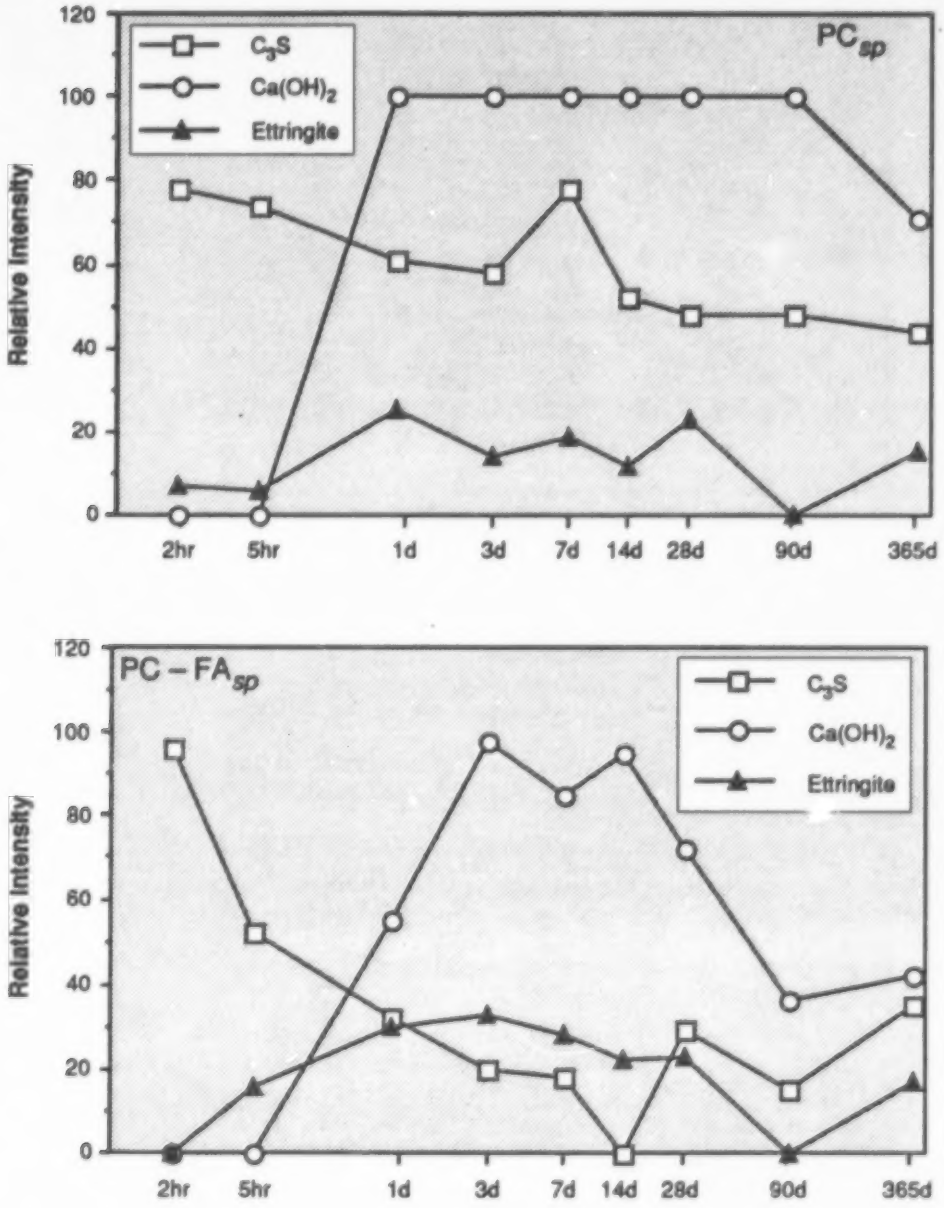

Figure 8. Variation of the relative intensities of major X-ray diffraction peaks for C_3S, $Ca(OH)_2$ and ettringite in the PC_{sp} paste (above) and PC-FA_{sp} paste (lower).

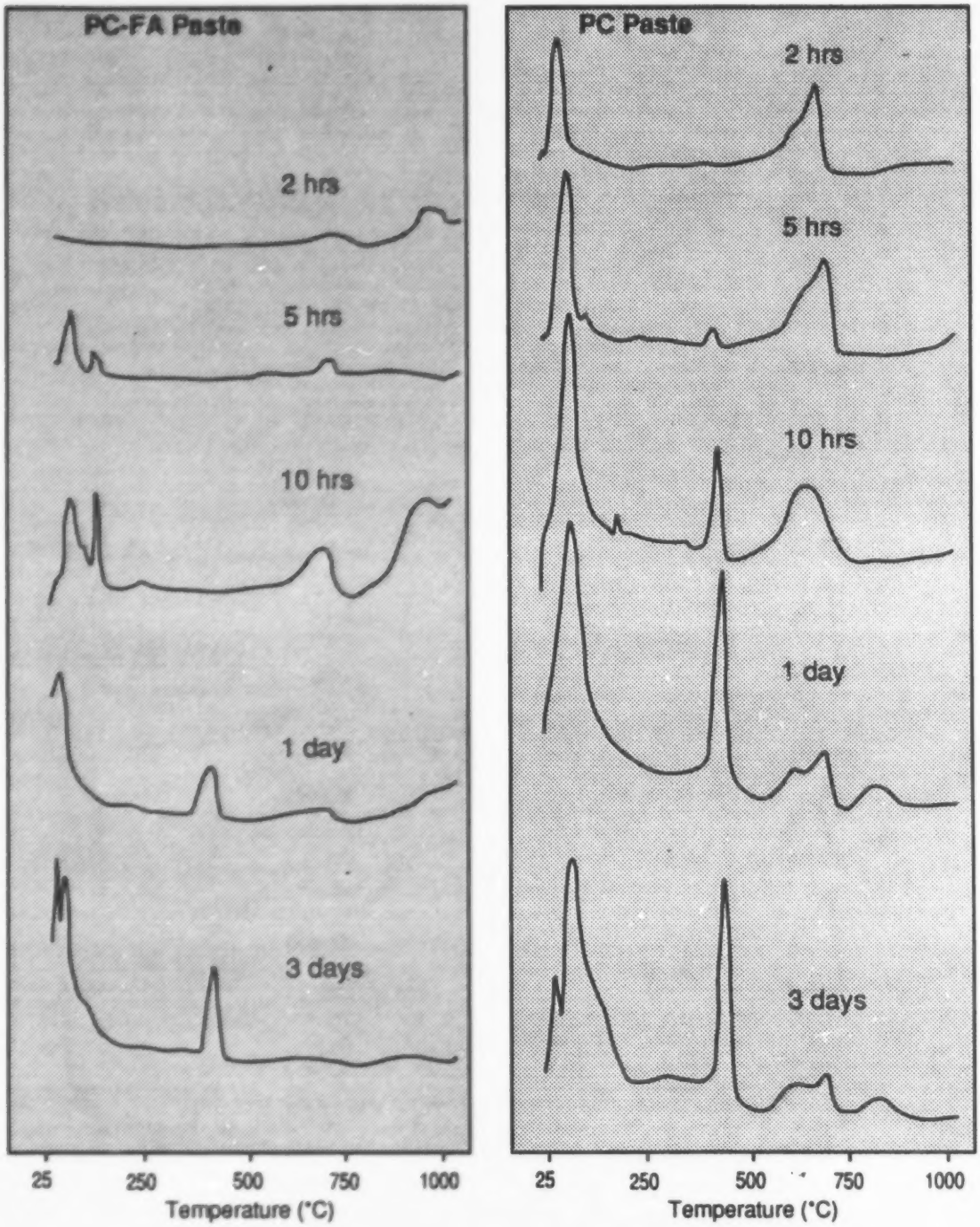

Figure 9a. Thermal curves (DTG) for PC and PC–FA pastes at early curing ages from 2h to 3d. Vertical scale is derivative weight loss and is the same for all curves.

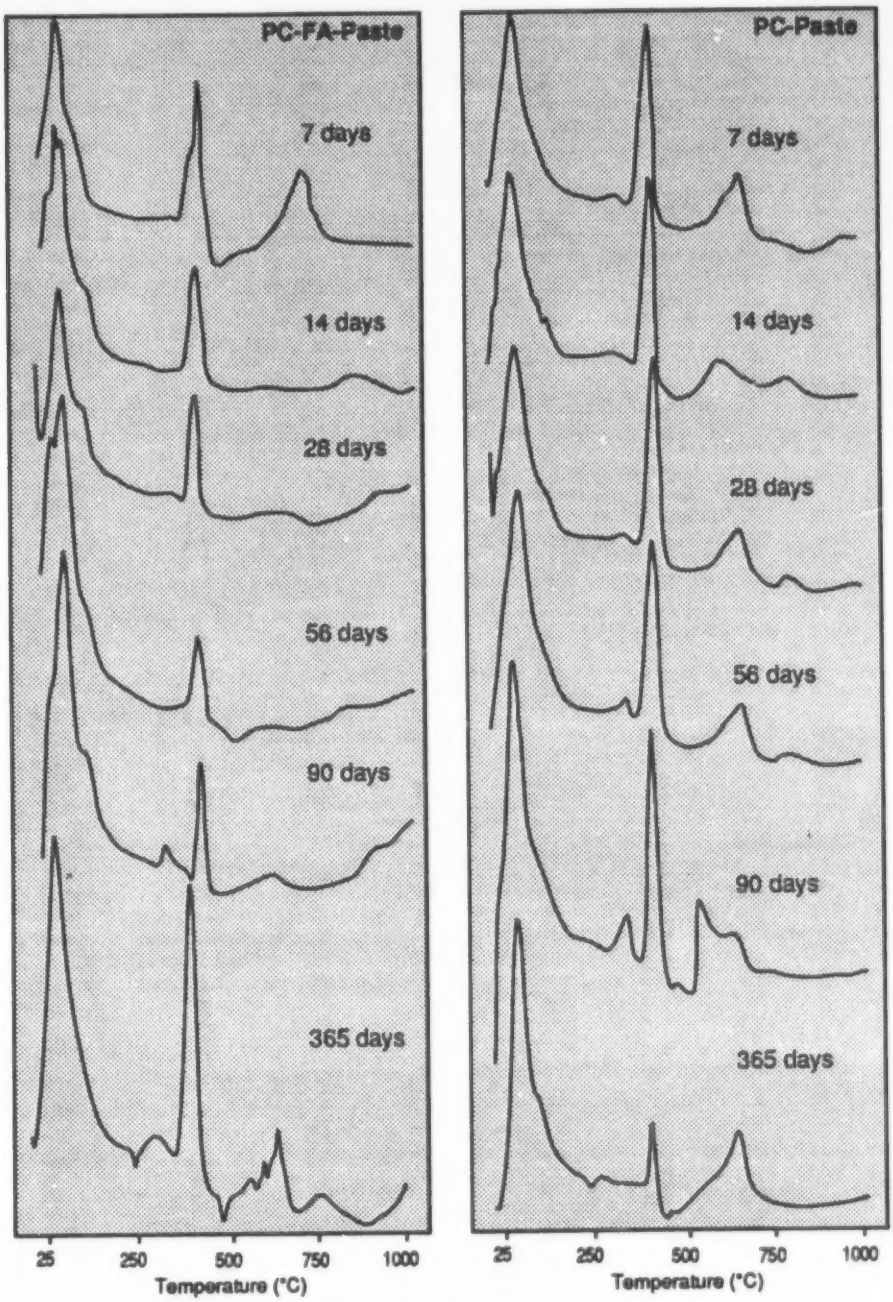

Figure 9b. Thermal curves (DTG) for PC and PC–FA pastes at curing ages from 7d to 365d. Vertical scale is derivative weight loss and is the same for all curves

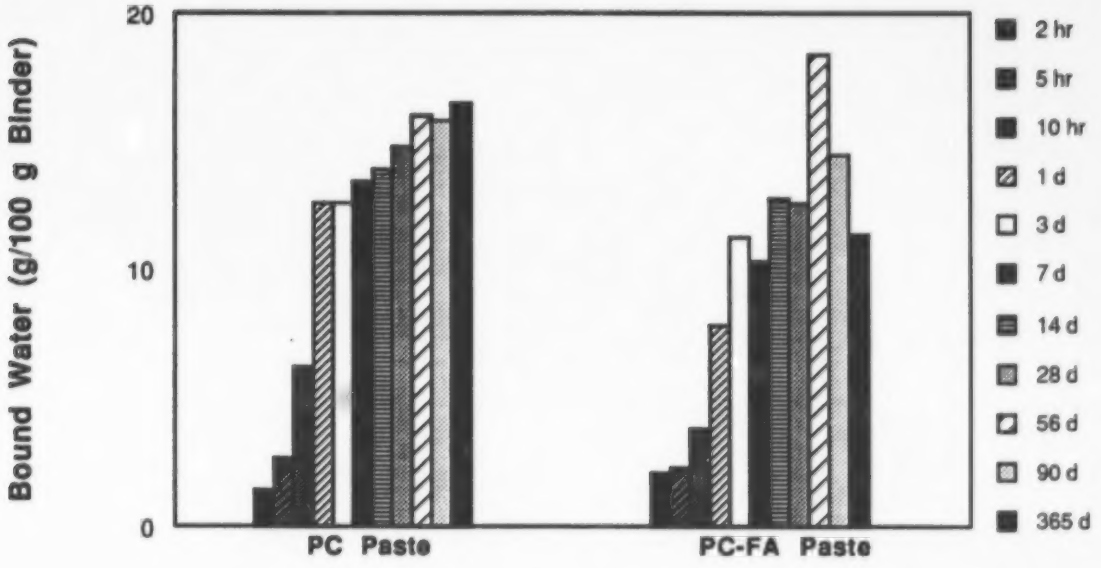

Figure 10a. Bound water contents (g/100g total binder) of PC and PC–FA pastes

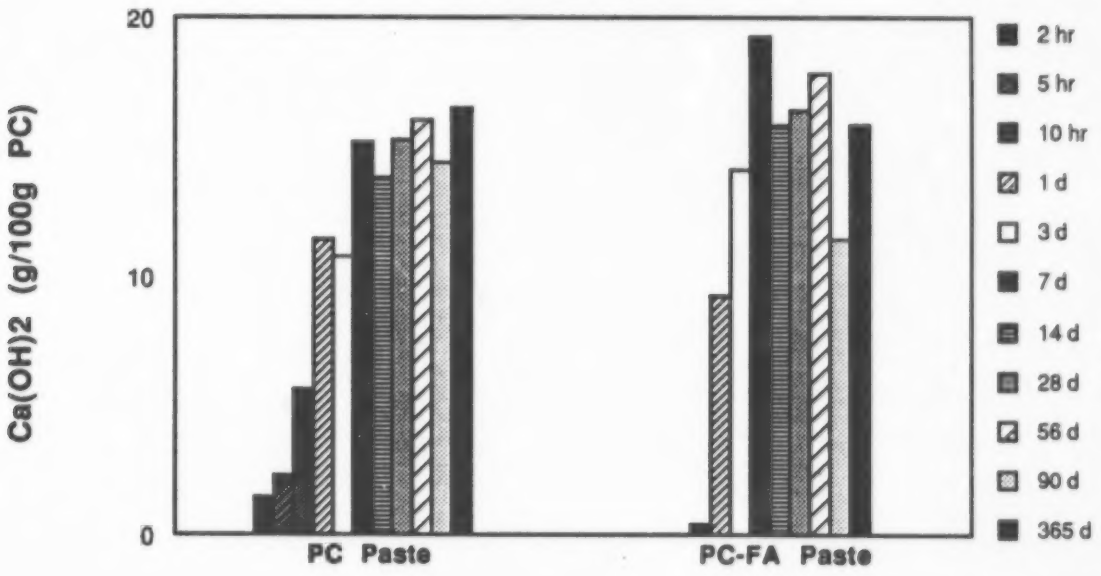

Figure 10b. Bound water contents (g/100g PC) of PC and PC–FA pastes

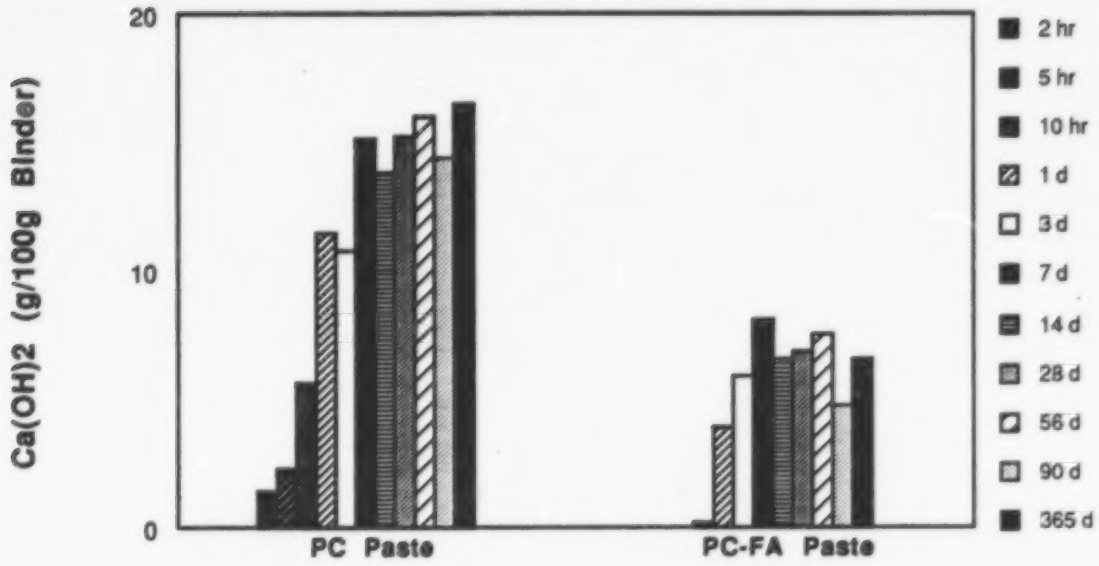

Figure 11a. Calcium hydroxide contents (g/100g total binder) of PC and PC–FA pastes

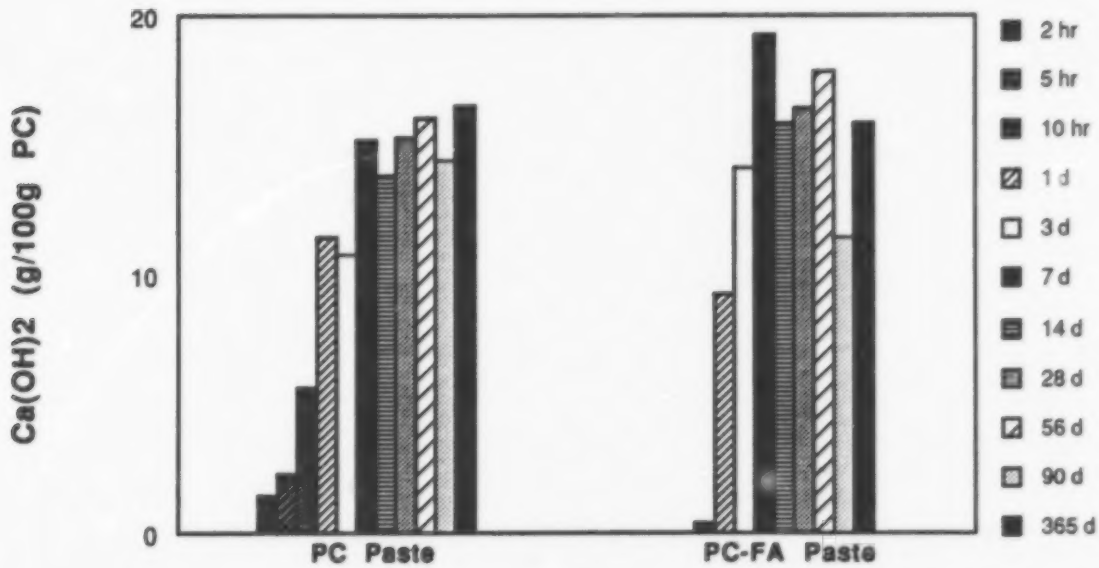

Figure 11b. Calcium hydroxide contents (g/100g PC) of PC and PC–FA pastes

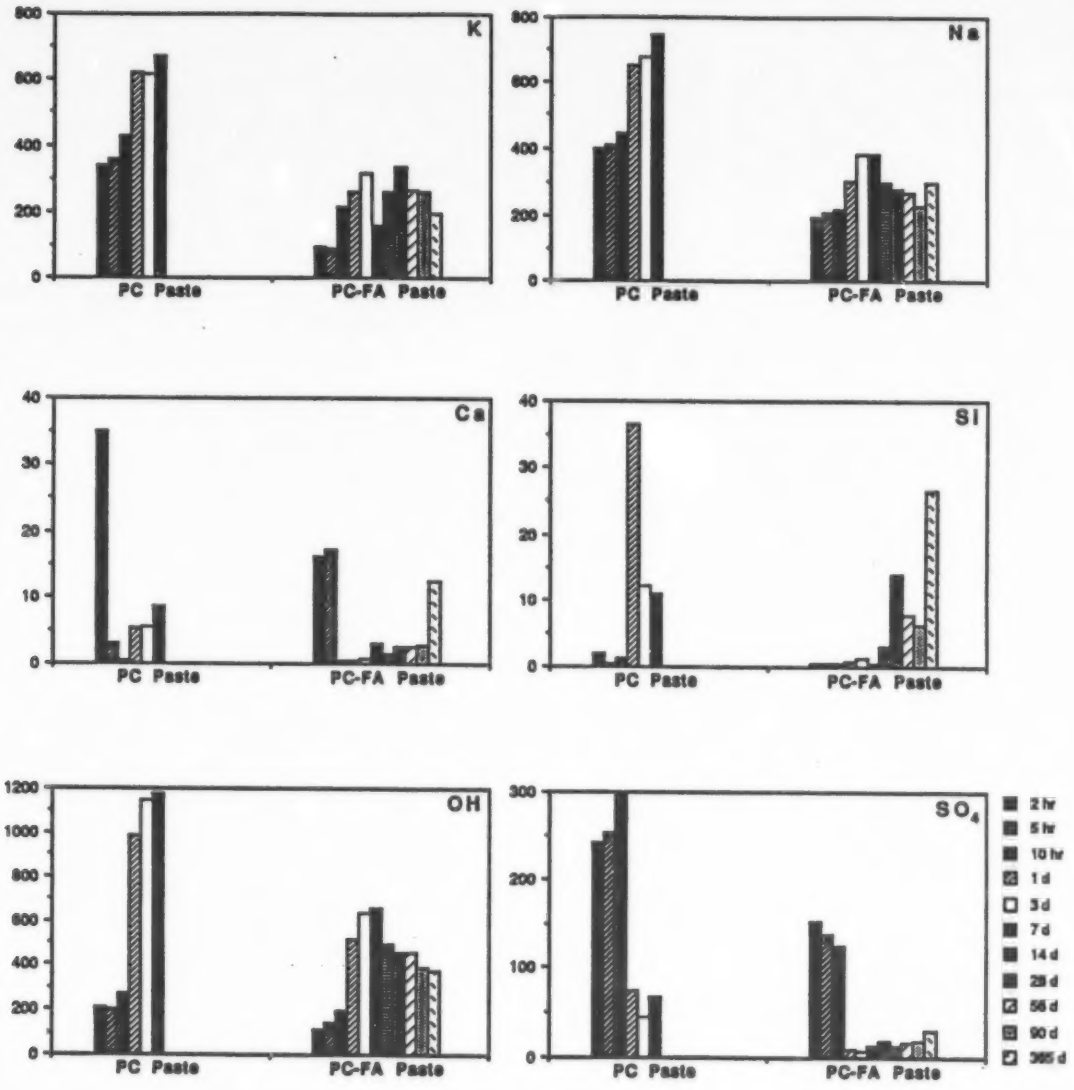

Figure 12. Variation in concentration of principal pore fluid ions extracted from PC and PC–FA pastes at curing ages from 2h to 365d. Vertical scale is mmol/L in each case.

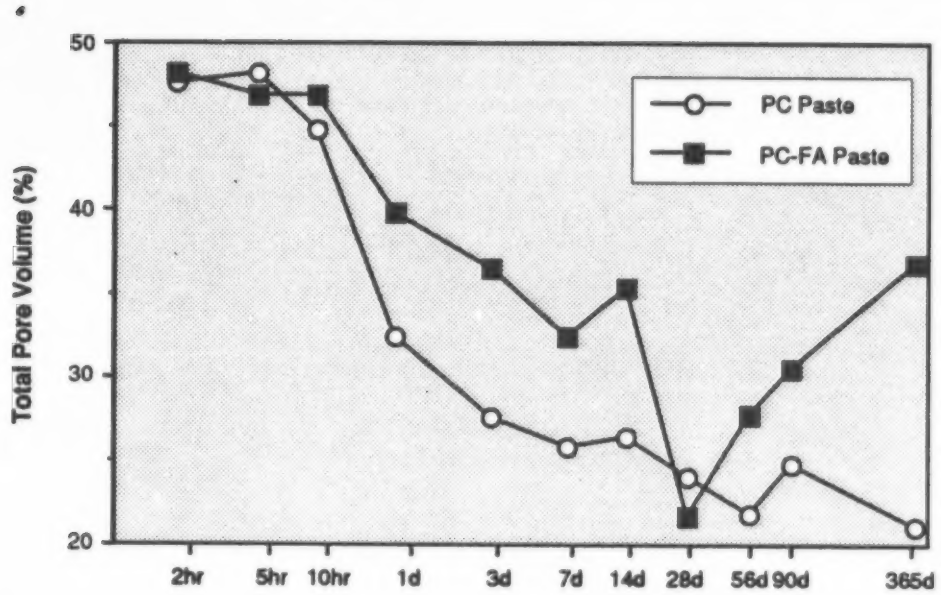

Figure 13. Variation in total pore volume (%) for the PC and PC–FA pastes at curing ages from 2h to 365d.

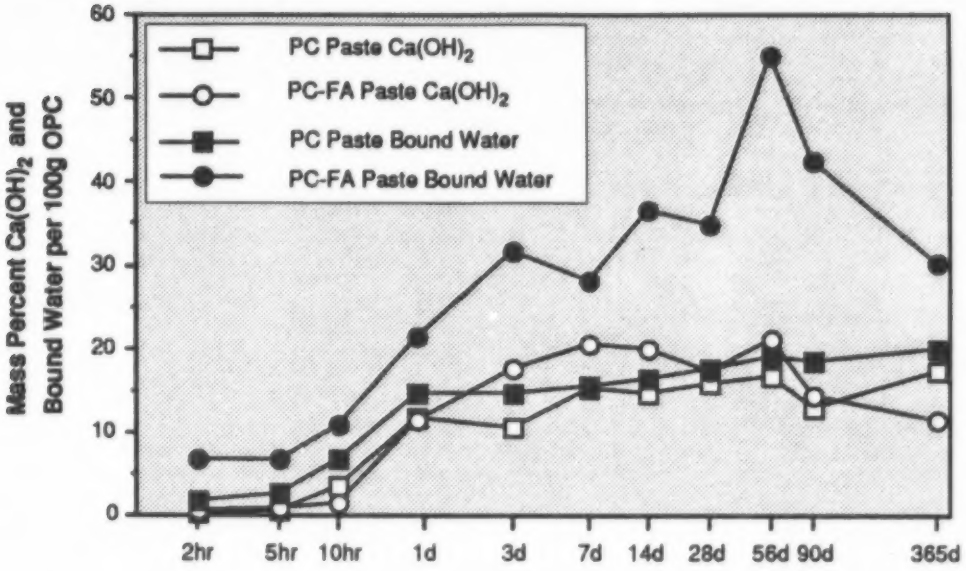

Figure 14. Variation of $Ca(OH)_2$ and bound water contents per 100g Portland cement for the PC and PC–FA pastes at curing ages from 2h to 365d.

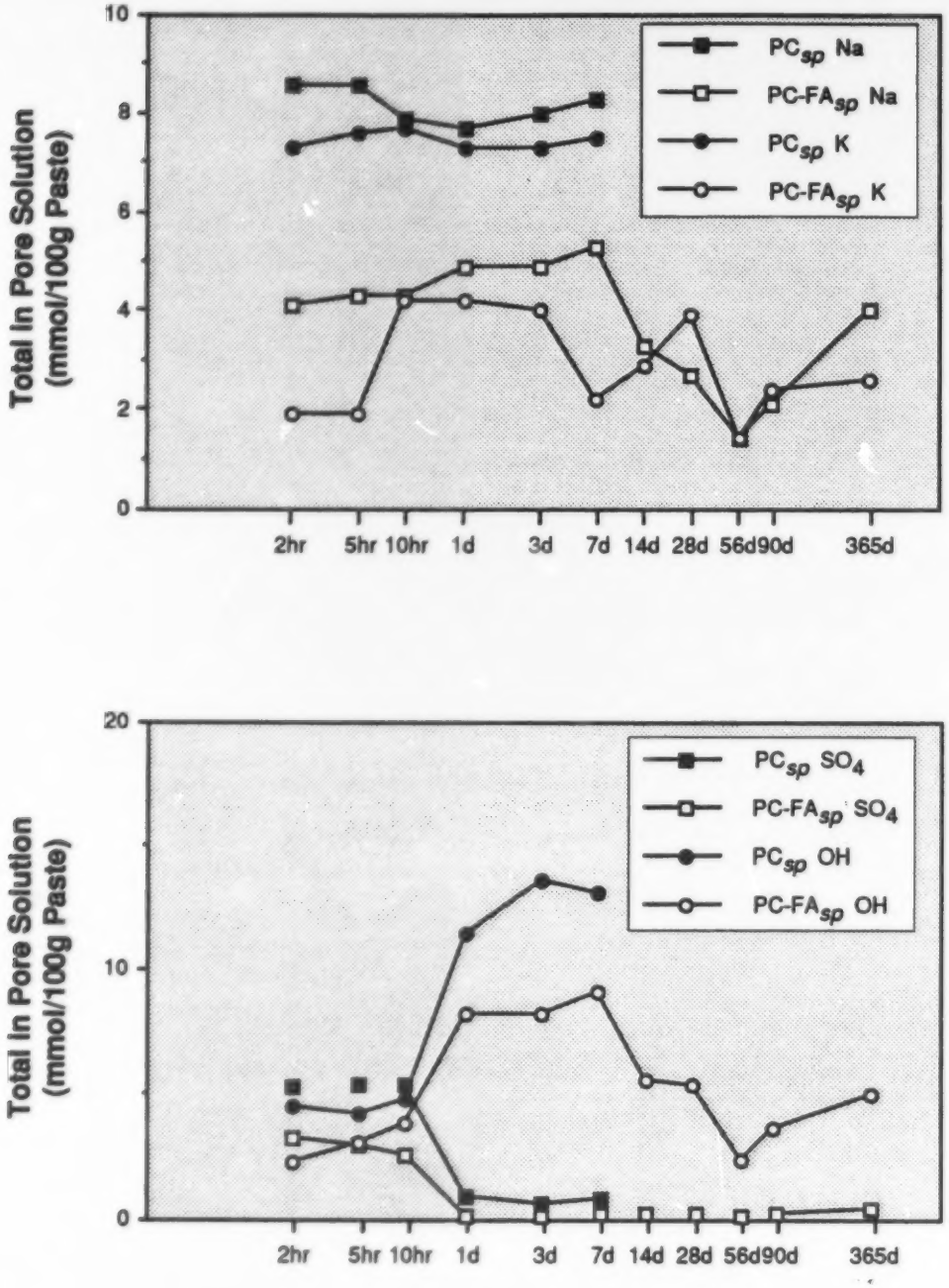

Figure 15. Concentrations of Na and K ions (top) and sulphate and hydroxyl ions (lower) extracted from PC and PC–FA pastes at curing ages from 2h to 365d (mmol per 100g paste).

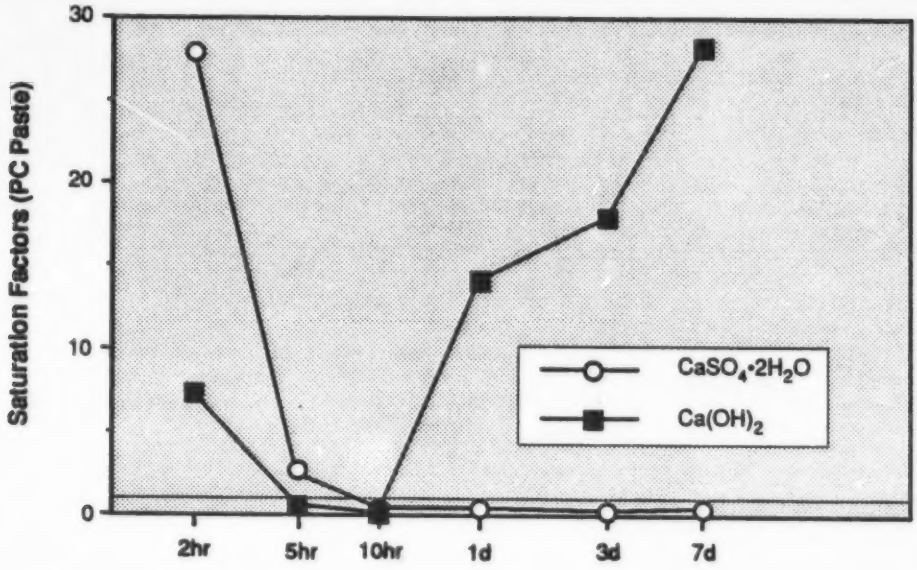

Figure 16. Variation of calculated saturation factors for pore fluid species in superplasticized Portland cement (PC) pastes with increasing curing age.

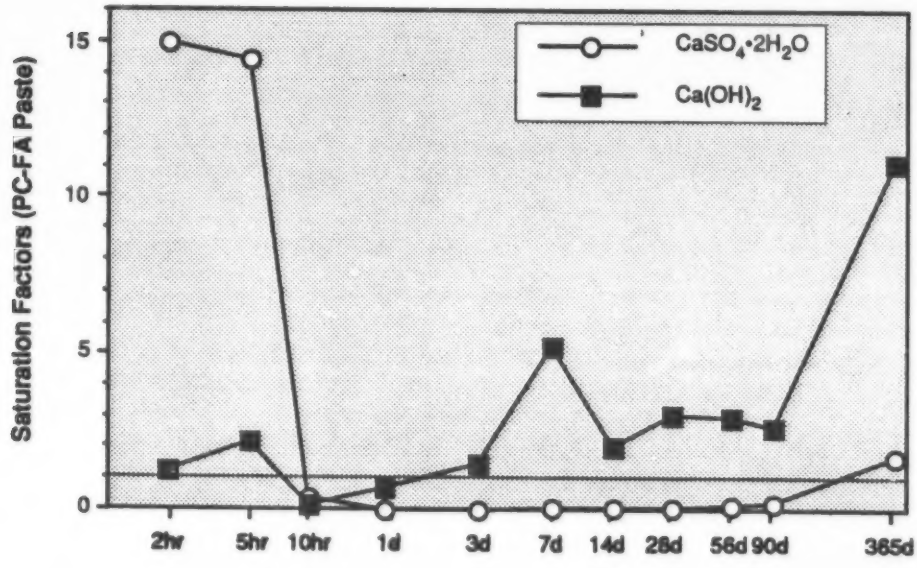

Figure 17. Variation of calculated saturation factors for pore fluid species in superplasticized Portland cement–fly ash (PC–FA) pastes with increasing curing age.

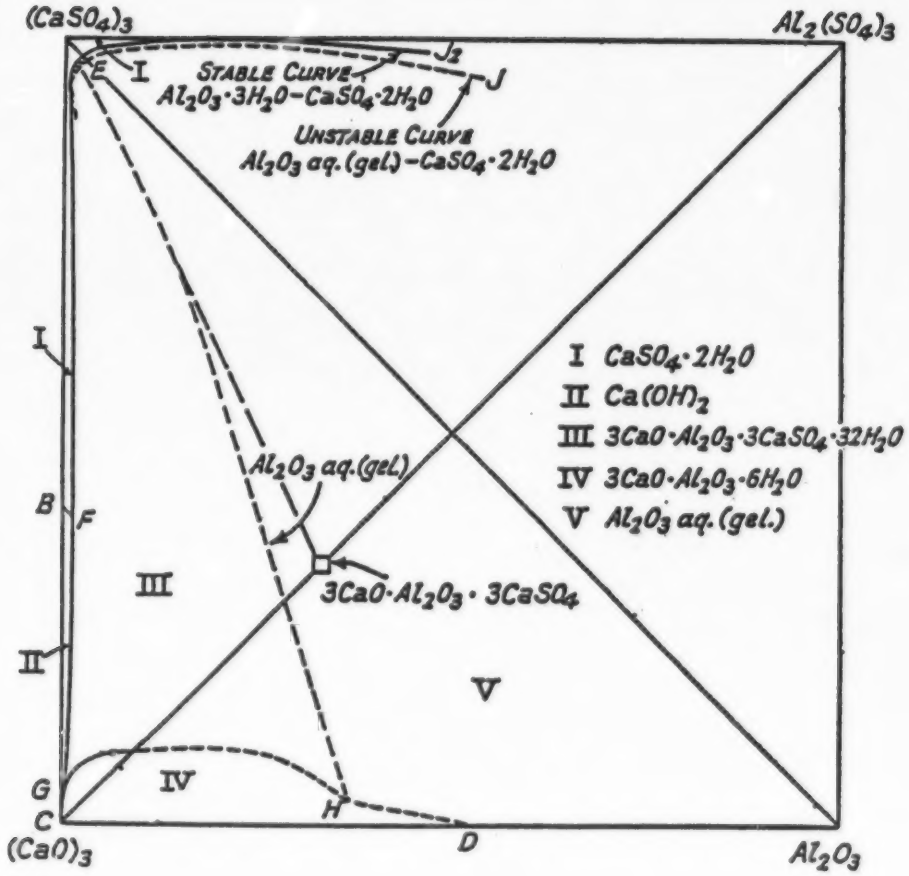

Figure 18. System $CaO–Al_2O_3–CaSO_4–H_2O$ simplified to conditions where $Al_2O_3.(gel)_{aq}$ is the source of Al_2O_3. Adapted from Lea (ref. 20)

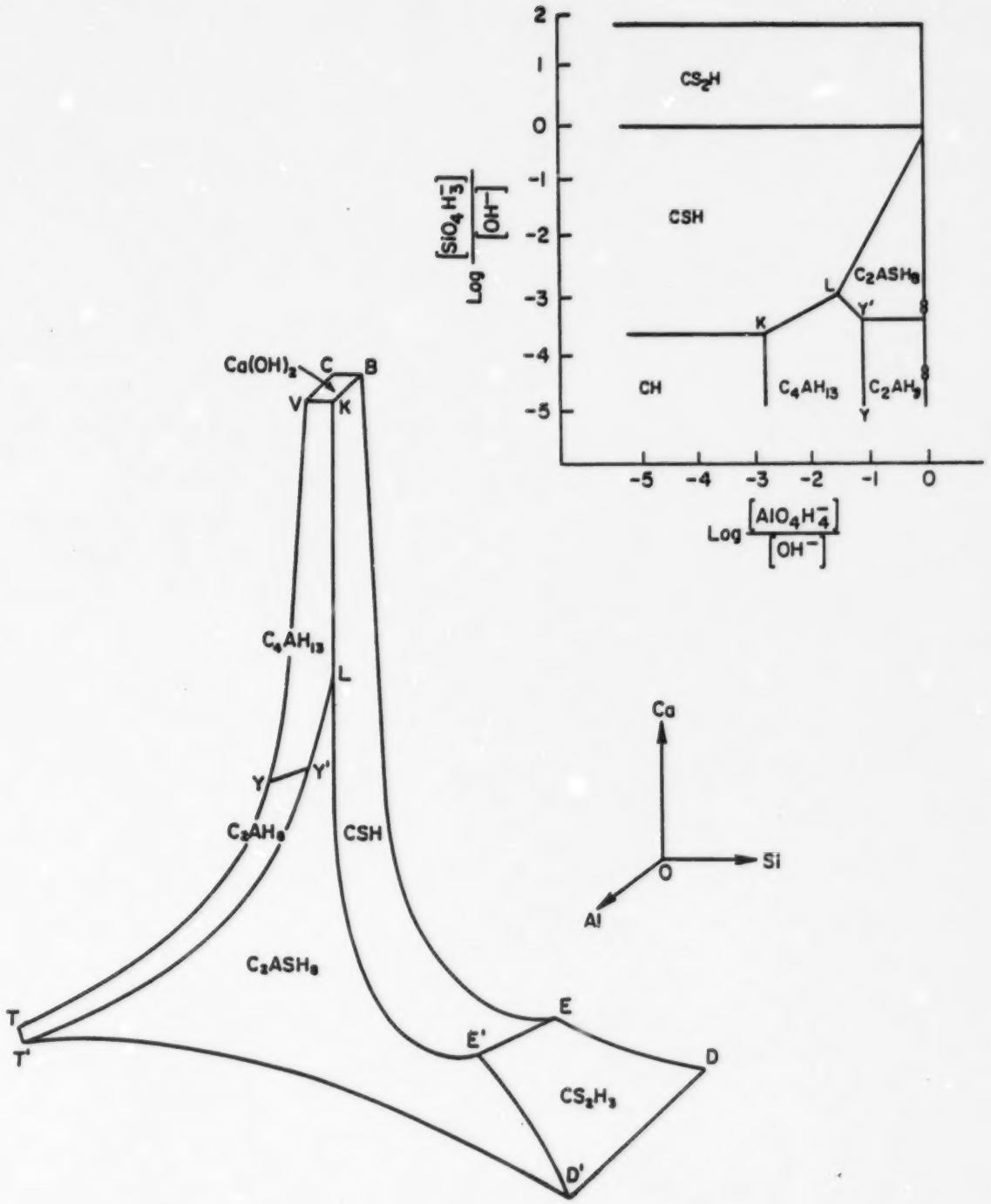

Figure 19. Phase equilibrium diagrams for the $CaO–Al_2O_3–SiO_2–H_2O$ system (32,33)

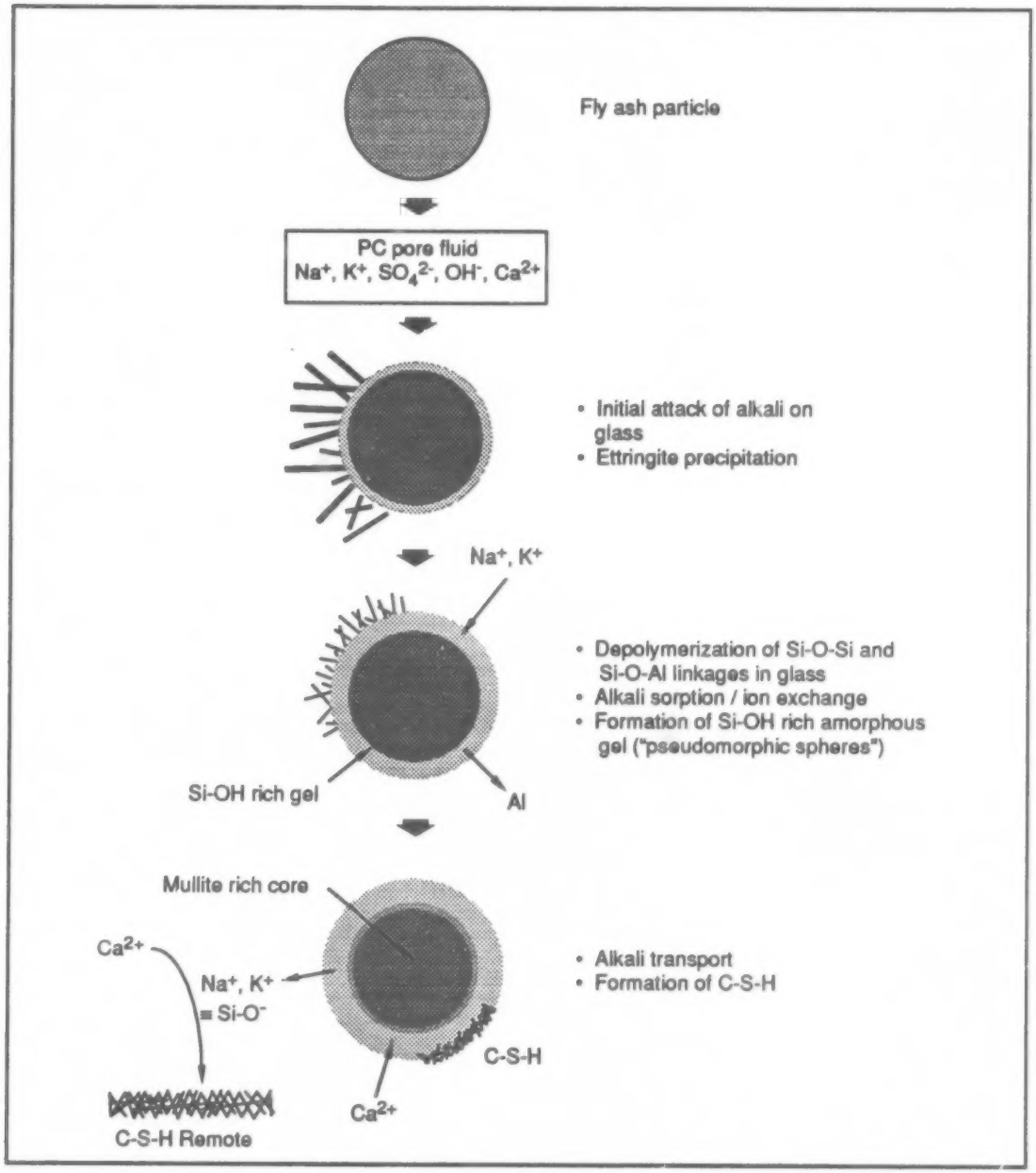

Figure 20. Model for the hydration reaction of fly ash in the presence of Portland cement.